Republic of Iraq
Ministry of Higher Education and Scientific Research
University of Misan / College of Engineering
The Department of Civil Engineering

STRENGTHENING AND REHABILITATION OF REINFORCED CONCRETE JOINTS USING POLYESTER BELTS

By

Dhiaa Chasib Rishq

B.Sc. in Civil Engineering, 2002

A thesis submitted in partial fulfillment of the requirements for the
Master of Science degree in Civil Engineering
The University of Misan

April 2021

Thesis Supervisor: **Prof. Dr. Abdulkhaliq Abdulyimah Jaafer**

بِسْمِ اللَّهِ الرَّحْمَٰنِ الرَّحِيمِ

﴿ يَرْفَعِ اللَّهُ الَّذِينَ آمَنُوا مِنْكُمْ وَالَّذِينَ أُوتُوا الْعِلْمَ دَرَجَاتٍ ۚ وَاللَّهُ بِمَا تَعْمَلُونَ خَبِيرٌ ﴾

صَدَقَ اللَّهُ العظيم

سورة المجادلة ﴿ الآية ١١ ﴾

DEDICATION

To my father's spirit, may GOD have mercy on him

My dear mother

My brothers and sisters

My family (my wife and children)

To all my friends and everyone who spared no effort to support me

I submit my effort to them with my respect and appreciation.

ACKNOWLEDGEMENTS

In the Name of Allah, the Most Gracious, the Most Merciful

I want to offer this endeavor to our GOD who helped me and enabled me to complete this research.

I would like to express my deepest gratitude grateful to my thesis supervisor Prof. Dr. Abdulkhaliq Abdulyimah Jaafer whom I had the honor of being under his supervision for his advice, continuous guidance and encouragement throughout this thesis.

I would like to extend my thanks to Prof. Dr. Abbas Oda Dawood Dean of the college of engineering, and Asst. Prof. Dr. Samir Mohamed Chassib, the Head of Civil Engineering Department.

I would like to express my thanks to Prof. Dr. Saad Fahad, Dr. Nasser Hakeem, Prof. Dr. Ahmed Khadim Al-Shara'a, Dr. Haider Abd Ali, Dr. Mustafa Chasib, Dr. Mohammed Muheibes, Mr. Hussein Sadiq and all the staffs of the materials laboratory for their technical support throughout the experimental program.

Special thanks and gratitude are due to my family and brothers for their care, patient and encouragement throughout the research period. Also special thanks to my Close friends.

ABSTRACT

In this study, a new suggested technique for strengthening and rehabilitation reinforced concrete joints using polyester belts was adopted. The current study aims to investigate the effect of concrete confining and concrete compressive strength on reinforced concrete joints. Moreover, the effect of strengthening and retrofitting of RC joint using polyester belt was studied. Three reinforcement details were adopted which are conventional reinforcement, reinforcement with internal closed stirrups and reinforcement with internal double closed stirrups. Three types of concrete were also used, normal strength, high strength and steel fiber reinforced concrete with compressive strength 43, 83 and 122 MPa, respectively. The test was carried out on fifteen specimens of reinforced concrete joints. The specimens were tested under a monotonic central point load as simply supported inverted (T-shaped) where the load was applied vertically downward on the face of the column. The strengthening was applied to two specimens while four specimens with different damage ratio (70 and 100) % were retrofitted. The test results showed that using reinforcement details with internal closed stirrups increased the ultimate load capacity for the joints specimens compared to the conventional reinforcement detail where the increasing was (47 and 50) % respectively for normal concrete, (44 and 47) % respectively for high strength concrete and 34% for steel fiber reinforced concrete. When the concrete compressive strength increased, the load capacity was increased too for both high strength and steel fiber reinforced concrete compared to the normal concrete for each reinforcement detail. For the conventional detail, the increase ratio for high strength and fibrous concrete was (16 and 66) % respectively, the increments were (13 and 51) % respectively when the reinforcement with internal closed stirrup was adopted while the

reinforcement with internal double closed stirrups achieved an increase of 13% for high strength compared to normal strength concrete.

As a result for using the polyester belts in strengthening and rehabilitation the joint specimens, the load carrying capacity has significantly increased by the range of (79 to 109) % compared to the non-strengthening specimen, respectively.

TABLE OF CONTENTS

LIST OF TABLES

LIST OF FIGURES

LIST OF SYMBOLS

F_t	Concrete tensile strength (MPa)
Fr	Concrete flexural strength (MPa)
F_{cu}	Concrete cube compressive strength (MPa)
f_y	Steel yield strength (MPa)
f_u	Steel ultimate tensile strength (MPa)
D_y	Deflection (mm) corresponding to 70% the ultimate load
μ	Ductility Index (unitless)
Δu	Ultimate deflection (mm)
Δy	Deflection at yield point (mm)

ABBREVIATIONS

RC	Reinforced Concrete
NSC	Normal Strength Concrete
HSC	High Strength Concrete
$SFRC$	Steel Fiber Reinforced Concrete
$I.Q.S$	Iraqi Standard
BS	British Standard
w/c	Water Cement Ratio
$ASTM$	American Society for Testing and Materials
ACI	American Concrete Institute
FRP	Fiber Reinforced Polymer
$CFRP$	Carbon Fiber Reinforced Polymer
$GFRP$	Glass Fiber Reinforced Polymer
NSM	Near Surface Mounted
FEM	Finite Element Model
$HRWR$	High Range Water Reducer
IS	Initial Stiffness
DI	Ductility Index

CHAPTER ONE

INTRODUCTION

1.1 General

In the current time, the earthquakes or seismic excitation have become a phenomenon that occurs from time to time which affects the performance of some reinforced concrete frame structures specially for the old building. During these events, many concrete frame buildings will be damaged and several people will lose their lives or homes.

The reinforced concrete frame structure that consists of reinforced concrete joints that have been designed according to the old requirements of the applied codes (without transverse shear reinforcement at the joint region) and before the application of the seismic requirements that are included in the new codes, it vulnerable to shear when undergo to seismic excitation. Then, the expected failure of such member is due to shear at the joint core. While the desired failure of those constructed according to the new seismic code may be a flexural failure in which the plastic hinge should be at the joint interface. The formation of the plastic hinges at the interface of the joint is critical due to its penetration to the joint core and its effect on the bond drop (Arowojolu et al, 2019).

Under a severe earthquake, there may be a large amount of shear stress concentrated at the region of the joint exceeding the shear capacity of the joint. Therefore, the brittle shear failure in the joint area may lead to serious consequences of severe damages and total collapse of the buildings (Le-Trung et al., 2010). Figure 1.1 shows the main failure mode of RC joint

(a) Joint shear failure

(a) Un adequate anchor

Figure 1.1 The main failure mode of RC joint (Singh et al, 2015)

1.2 Reinforced Concrete Joint

A joint is defined as that portion of the column within the depth of the deepest beam that frames into the column. In the RC frame structure, three kinds of RC beam - column joint can be observed. The first one is the interior joint that consists of four beams attached the vertical faces of the column. The second is the corner joint. It includes two beams attached two adjacent vertical faces of the column. The third one is the exterior joint that contains two beams attached to two parallel vertical faces of the column and beam attached to the face of column perpendicular to them (ACI 352R-02) . Figure 1.2 shows these kinds of joints.

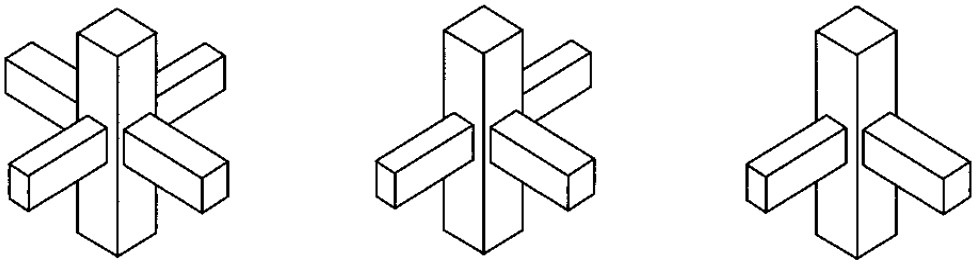

(a)Interior (b) Exterior (c) Corner

Figure 1.2 Types of RC joints (ACI 352R-02)

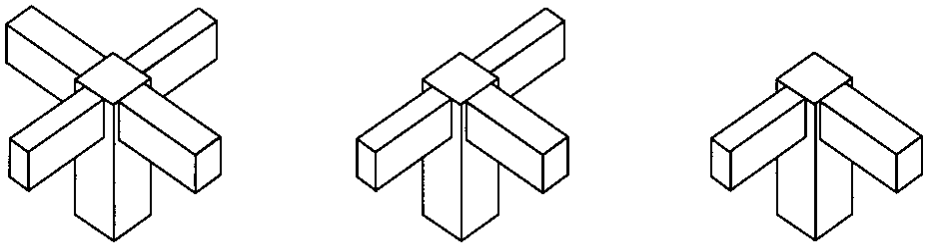

(d)"Roof"-Interior (e) "Roof"- Exterior (c) "Roof"-Corner

Figure 1.2 : Continued

1.3 Forces Acting to the RC Joints

Under an earthquake action, an asymmetric and cyclic bending moment diagram takes place due to the dynamic effect of loading and unloading. The bending of the structure against horizontal forces are distributed according to Figure 1.3

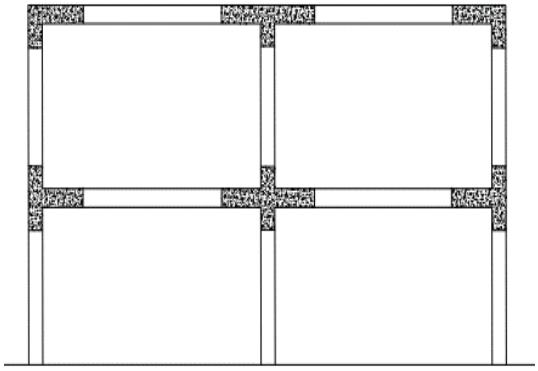

(a) The structure before earthquake

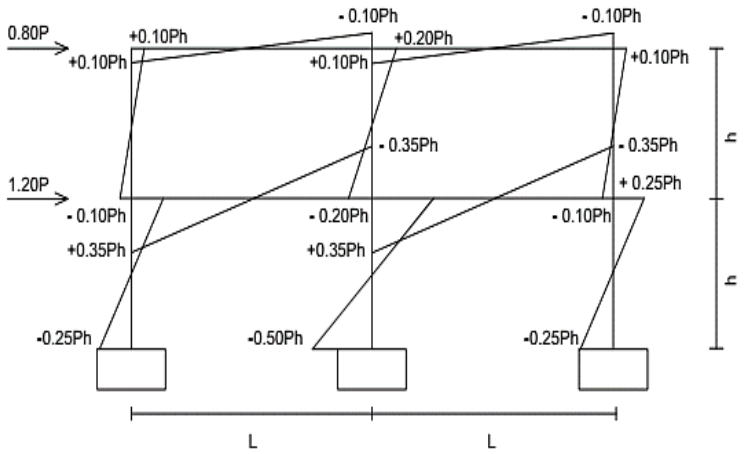

(b) The structure subjected to earthquake

Figure 1.3 Bending of the structure under the earthquake effect (Montava et al., 2019)

The effect of load on each of the three kinds of these joints is explained with concerning the stresses and the related cracks developed at them. The forces that effect on interior RC joint under gravity load are illustrated in Figure 1.4 (a). The axial force from the column, tension and compression forces from the beam directly can be transmitted to the joint. In case of lateral load applies to the joint as shown in Figure 1.4 (b), diagonal compressive and tensile stresses at the joint area will increase and the cracks development will be perpendicular to the tension diagonal A-B at the joint as well as on the face of column intersecting the beam. Both ties in tension and struts in compression are represented by solid and dashed lines respectively, where the concrete is weak in tension, thus transvers reinforcement used to cut the plane of failure for resisting the diagonal tensile forces. For exterior joint, the reinforcement is required at the joint region to resist the cracks that will develop at the joint region due to the shear force. So, the efficiency of this type of joint depends on the longitudinal reinforcement details. Figure 1.5(a) clarifies the forces that act on the exterior RC joint. Both Figure 1.5 (b) and 1.5 (c) show the typical details for the reinforcement at the joint region. The efficiency range that will obtain by passing and bending the steel bars at the core of the joint is (85-100) % as shown in Figure 1.5 (c). However, bending the steel bars away from the joint core will achieve efficiency range (25-40) % as shown in Figure 1.5 (b). Closed stirrups must be used for confining the concrete a core. Figure 1.6 illustrates the forces that effect the corner RC joint with continuous column over the joint. Understanding the force that affected on the corner joint will be in the same way in exterior joint concerning the load direction (binti Abd Kader et al., 2019; Uma & Prasad, 1996). An exterior RC joint will be investigated at our current study.

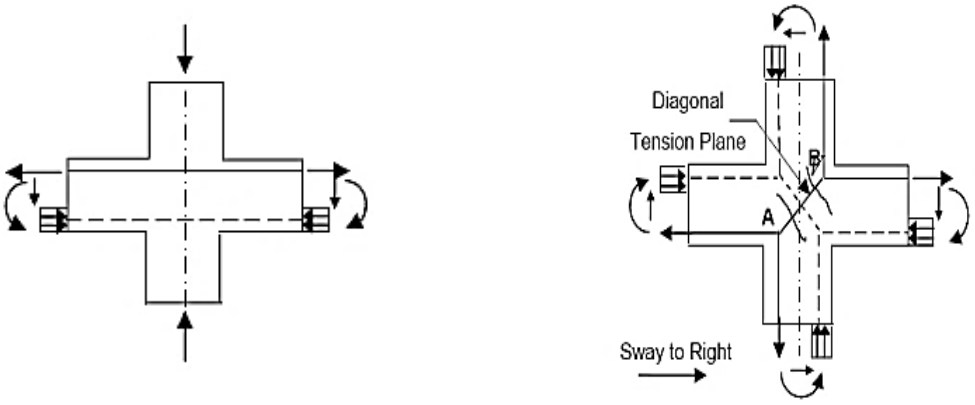

(a)Gravity load (b) Seismic load

Figure 1.4 Interior joint (binti Abd Kader et al, 2019)

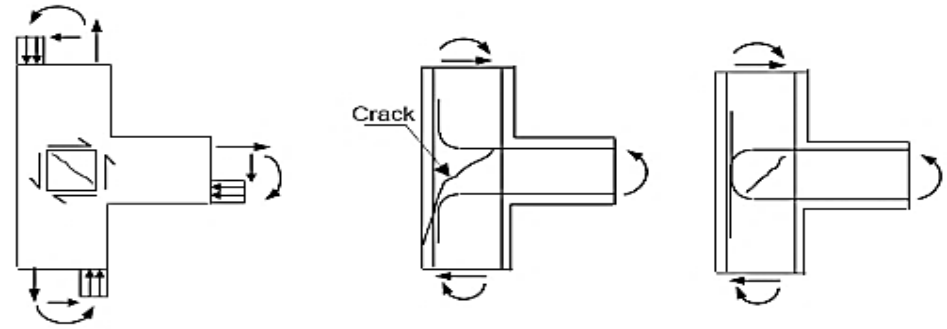

(a) Forces (b) Poor detail (c) Satisfy detail

Figure 1.5 Exterior RC joint (binti Abd Kader et al., 2019)

Figure 1.6 Corner RC joint (binti Abd Kader et al., 2019)

1.4 Webbing

Webbing is a strong multi-purposes woven fabric. It is used usually instead of ropes, steel wires and the metal chains in the everyday life for industrial and other purposes. It is available in different types differ in shape, length, width, color, strength and it classify according to the type of fibers that include. There are many types of the synthetic fibers such as (Fangueiro, 2011):

(a) Polyester
(b) Cotton.
(c) Nylon.
(d) Polypropylene.
(e) Aramid.
(f) Carbon

A polyester webbing will adopt for strengthening and retrofitting of the reinforced concrete beam - column joint.

1.4.1 Polyester Webbing

Polyester webbing is one of the most common kinds of webbing use in different industries. it has a set of benefits more than some types of webbing. Where it is widely used in our life due to its cheap price, lightweight, available at the local market and also for its excellent strength. It is a flexible webbing and has the ability for wrapping tightly around the surface. It is used for lifting or pulling the heavyweights such as concrete blocks, pipelines, it is easy adhesion when it is used with epoxy for strengthening and retrofitting works, it doesn't need a long time for curing and it is also doesn't need skilled workers to apply. Figure 1.7 shows the polyester webbing. Some characteristics of this polyester webbing are (Fangueiro, 2011):

(a) Initial modulus (10.2-10.6) N/tex.

(b) Resistant to stretching and shrinking.

(c) Abrasion resistance.

(d) Moisture: has a very low regain of 0.4%.

(e) Melting temperature (258-263) C^{o}.

(f) Resistance to most chemicals.

(g) Polyester has excellent resistance to sunlight (one of the best for outdoor use).

(h) Specific gravity :1.38.

(i) Tenacity: 0.62- 0.85 N/tex.

Figure 1.7 Polyester webbing

1.5 Steel Fiber Reinforced Concrete

Fiber Reinforced Concrete (FRC) can be defined as a composite material basically containing a normal concrete or mortar randomly reinforced by discrete short fibers. The fibers are usually fabricated from plastic, steel, glass, and other materials. Steel fibers can be defined as separated, short length steel of aspect ratio in the range (20-100) and that are quite small to be easily dispersed randomly in the mix of fresh concrete mix. When a steel fiber is used at this concrete, the produced concrete mix namely

Steel Fiber Reinforced Concrete (SFRC) (Behbahani et al, 2011). Many benefits are obtained from using steel fiber. They are as follows:

(a) increase the resistance of impact and spalling.
(b) Prevent the growth of the crack and widen under the service load.
(c) Enhance the ductility of the structure under the seismic load.
(d) Enhance the shear and flexural strength.
(e) Enhance the toughness

(SFRC) composition consists of cement, fine and coarse aggregates, water, and steel fiber. The behavior of (SFRC) can be classified according to the application and the amount of fibers as a percentage of the total volume of concrete into three sets. The first set is of a very low volume fraction of steel fiber 1% that has been used for a long time to control plastic shrinkage and as pavement reinforcement. The second set is of moderate volume fraction of steel fiber (1 to 2) % which can be used to enhance modulus of rupture, impact resistance, and toughness in addition to other eligible mechanical characteristics of concrete. While the last set is of a high-volume fraction of steel fiber more than 2%, these include the SIFCON and it is used for special purposes like blast and impact resistance. SFRC is used for different purposes such as the Highways and pavements of airports, hydraulic structures, fiber shotcrete…etc. (Behbahani et al, 2011)

1.6 High Strength Concrete

The concrete for a long time has represented the main material for supplying a firm and safe infrastructure. The concrete with compressive strengths range of 20 - 40 MPa has been widely used in construction projects. Long-term poor performance of a normal concrete drove to encourage the researchers for the development of concrete with specification better than the conventional concrete concerning the durability, workability and

affordability. Thus, it enabled to construct an economical and sustainable structures with developed architectural shapes. Produce and develop high strength concrete HSC has been a great step in the concrete technology. High strength concrete is defined as concrete with a specified compressive strength of 55 MPa or higher (ACI 363R, 2010). High strength concrete is used in engineering projects that have concrete members that must be strong against high compressive loads. High strength concrete contains in its composition cement, aggregates, low water to cementitious material, superplasticizers and silica fume or fly ash. HSC is typically used in the high - rise building, highway bridges, dams… etc. (Revanth Jagana, 2017)

1.7 Objectives of the Research

The main objectives of this research are to investigate the behavior RC joint as follows:

1. To study the effect of confining concrete at the joint core by using internal closed stirrups and addition steel bars.
2. To investigate the effect of concrete compressive strength on the ductility characteristics of the joint by using three types of concrete.
3. To study the effect of strengthening and rehabilitation of RC beam - column joint of partial damage (70% of its ultimate load) and fully damage (100% of its ultimate load) using polyester webbing as a new suggested technique.

1.8 Organization of the Thesis

The thesis consists of five chapters. They are as follows:

Chapter One **:** Represents a general introduction about the concept of RC joints and the force acting on it, polyester webbing, high strength concrete, steel fiber reinforced concrete and the objectives of research

Chapter Two **:** In this chapter, a review of some previous studies related to the strengthening and rehabilitation of reinforced concrete Joints using different techniques has been included in addition to the summary.

Chapter Three **:** The specification and testing results of the materials used in this study, instrumentation, the tests and the mixing quantities of the concrete. The steps of work, the joint specimens' details, the method of preparation, casting and the test procedure are illustrated in this chapter**.**

Chapter Four **:** The results of the experimental program and discussion of the obtained results are included in this chapter.

Chapter Five : Explanation of the important conclusions that were reached from the obtained results during this study. Some recommendations and proposals for further studies were included too.

CHAPTER TWO

LITERATURE REVIEW

2.1 General

Researches and studies are conducted in the past few decades were aimed at studying the strengthening and rehabilitation of reinforced concrete joints. Different materials with different techniques were used. This chapter summarizes the most important and recent experiences and developments on which researchers worked and reviewed their results in this field.

2.2 Strengthening of RC Beam - Column Joint

There are many common ways for strengthening the critical region of the reinforced concrete beam column joints in the concrete frame buildings. These ways can be divided into two groups which are respectively: interior and exterior strengthening. The first one includes using advanced reinforcement steel detail, fiber reinforced concrete, SIFCON, high strength concrete and so on, while the second includes jacketing (concrete, steel, fiber reinforcement polymer (FRP), ferrocement) or composite jacketing ...etc. This chapter includes some of the available experimental and/or theoretical researches that are related to strengthening of the reinforced concrete beam column joint.

2.2.1 Strengthening by Jacketing

It is one of the strengthening methods used to enhance the capacity of different concrete member (beam, column, beam-column joint….). Various materials can be used in this technique to perform the intended purpose when used to strengthen structural elements such as concrete, steel, carbon fiber reinforced polymer CFRP, glass fiber reinforced polymer GFRP, SIFCON…etc.

2.2.1.1 CFRP and GFRP Jacketing

Attari et al. in 2010 investigated the effect of fiber reinforced polymer (FRP) strengthening on the efficiency of beam - column joint subjected to reverse cyclic load. In this study, the test was carried out on three specimens. The first was considered as a control specimen. The dimensions of control specimen were the same with respect to cross section area for both column and beam (0.15×0.1) m while their length was 0.75 and 1.35 m respectively. The two remaining samples were the same dimensions and details of the control, one of them was strengthened with Carbon Fiber Reinforced Polymer (CFRP) plate on upper and lower face of beam while the rehabilitation scheme had been done on the other using single layer of CFRP sheet, two L-shaped layers of Glass Fiber Reinforced Polymer (GFRP) on upper and lower face of beam as well as two layers of GFRP wrapped on the column. The results showed that the ultimate load of the repaired specimen using of hybrid fibers (GFRP sheets and CFRP plates) was increased by 44% and the ductility was improved by 23% compared to the control specimen.

An experimentally study was achieved by **Le - Trung et al.** in 2010, they studied non-seismic reinforced concrete joint strengthened by carbon fiber reinforced polymer to improve the lateral strength and ductility of non-seismic RC beam-column joint. The test was conducted on eight specimens which represented an exterior reinforced concrete joint. Six specimens of them have been retrofitted with various arranging shapes of CFRP sheets and/or strips as shown in Figure 2.1 . One of the remaining two samples represented non seismic behavior and the other had a seismic detail. The result of the study showed that using of CFRP with suitable arranging (X shape) enhanced the lateral strength of the non-seismic specimen by 17.5% and the ductility was increased by 5.3 times compared to the non-seismic specimen. Also, using double layers of CFRP gave a great enhancement of

the ductility as well as to the lateral strength where they increased by 3.6 times and 31.7%, respectively.

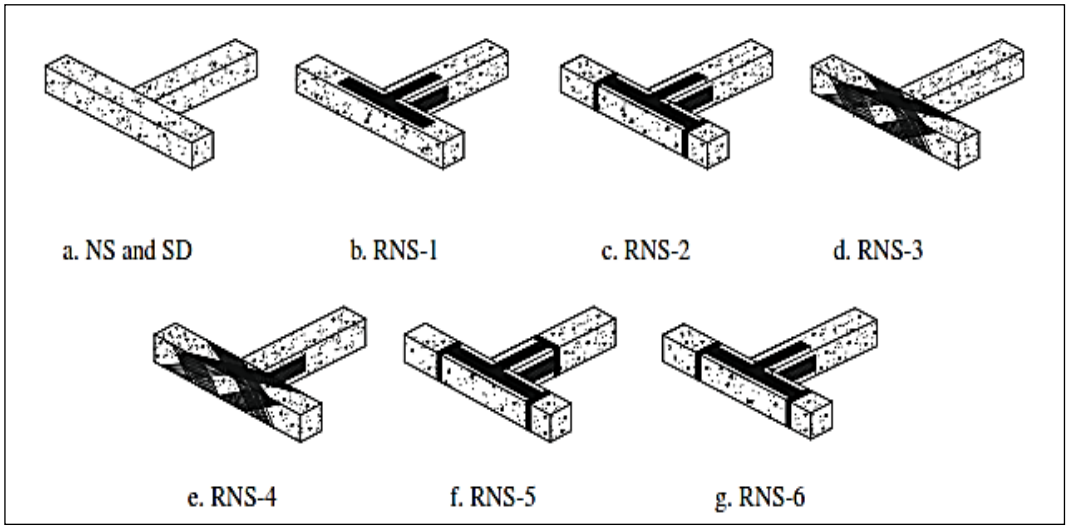

Figure 2.1 Description of all tested specimens (Le - Trung et al.)

Mahmoud et al. in 2014 experimentally studied the rehabilitation of exterior reinforced concrete beam column joint using CFRP technique. In this study, the test was conducted on eleven specimens. One specimen represented the control. The ten specimens remained were divided into three sets have been casted to cover three likely failure modes. The first set included three specimens represented the first defect which was the absence of the stirrups at joint core. The second set included three specimens represented the defect of insufficient bond length for the beam main steel reinforcement while the last set had four specimens represented the third defect that was deficiently executed implanted column on an old one. For both set1 and 2, two strengthening configurations were suggested while three configurations were considered for set 3. Three styles of strengthening were used for rehabilitation of the reinforced concrete joint including strips, sheets and near-surface mounted NSM strips of CFRP as shown in Figure 2.2 .

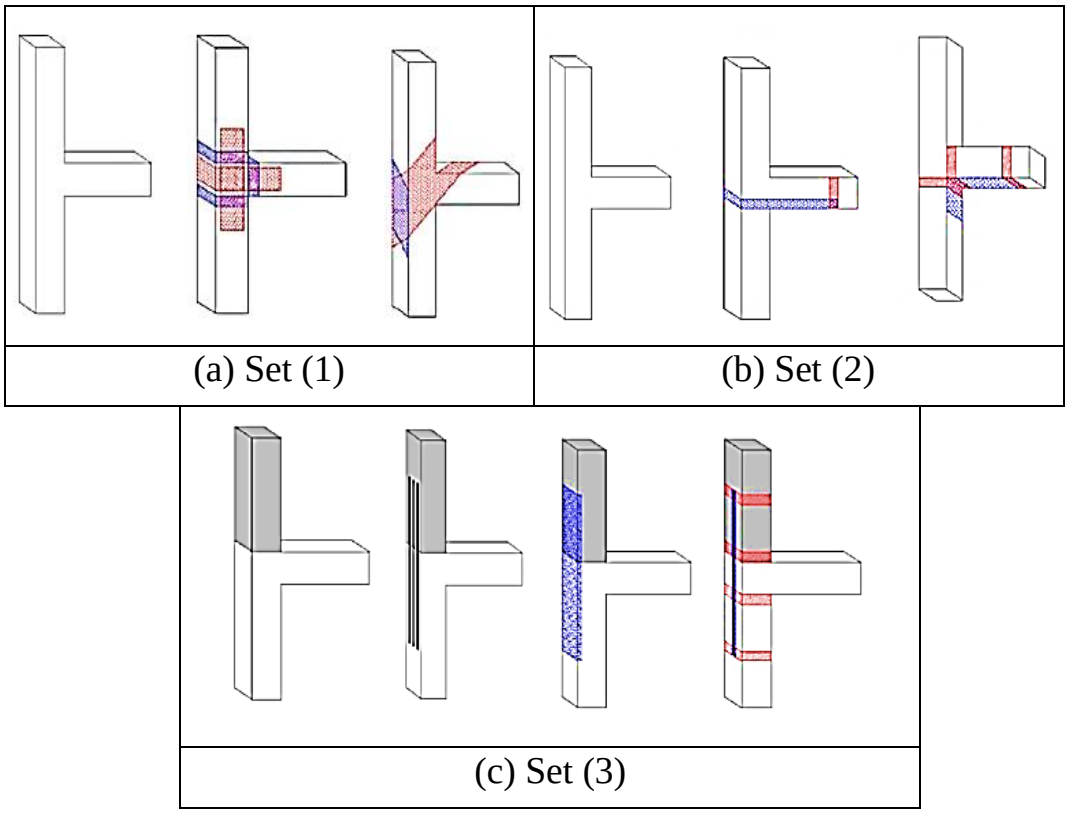

Figure 2.2 Strengthening Schemes of tested specimens
(Mahmoud et al., 2014)

The results explained that the suggested pattern of the CFRP strengthening were the best option for strengthening the first two failure modes. The diagonal sheets at the first set were the better choice for preventing the failure of the joint has no stirrups while the (L-shaped) sheets at the second group were adequate for resisting the failure of specimen had insufficient bond length of the main steel bars in beam. However, third set results explained that using NSM strips method enhanced the structural behavior of the specimen where the load capacity increased by 6.6% compared to the control specimen. Moreover, using bonded CFRP sheets and strips failed to improve the joints capacity. The failure of the third group was due to splitting of the upper implanted column and peeling off of either CFRP NSM or CFRP sheet or rupture of the anchorage U shaped layer.

Hadi and **Tran** in 2016 applied a new strengthening technic on exterior reinforced concrete beam - column joint by using both CFRP and circular concrete cover to strengthen the joint as shown in Figure 2.3.

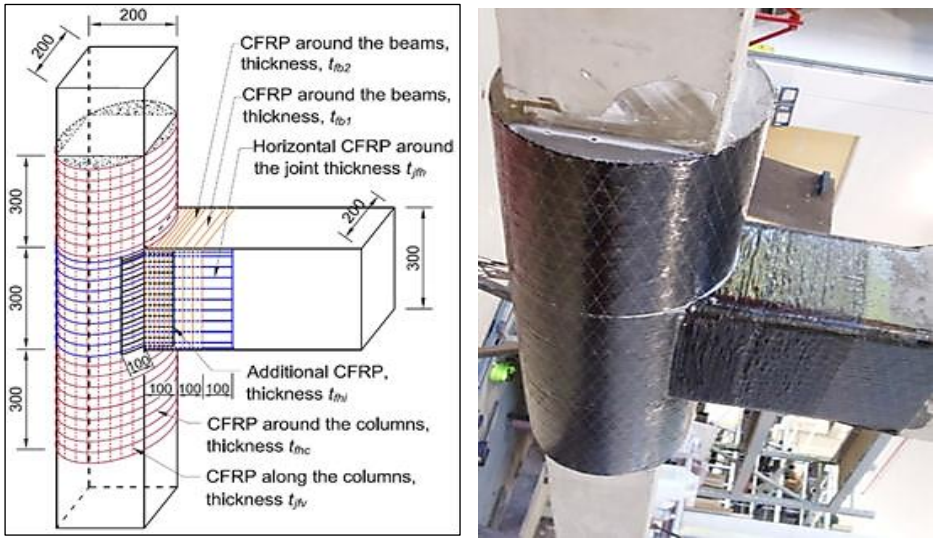

(a) CFRP scheme (b) Strengthening scheme

Figure 2.3 Strengthening using CFRP and circular concrete cover (Hadi and Tran, 2014)

Four RC beam - column joint specimens were casted. The first one represented the reference specimen while the other remaining three specimens were strengthened by surrounding the square column by circular concrete cover at the joint region then CFRP sheets were wrapped on the column and beam with different thickness. The procedure of strengthening was implemented in two stages. At the first stage, surrounding the columns of the specimens by circular concrete covers while the second stage included applying the CFRP sheets to the specimens according to the strengthening scheme. The samples were tested under cyclic load. The test results proved that the proposed strengthening method effectively improved the seismic performance of the joint. This method improved the CFRP confinement effect and prevented the debonding of the CFRP at the joint area, leading to the improvement in the effectiveness of the applied CFRP. Also, the results

showed that the fourth specimen that was strengthened with CFRP of 0.66 mm thick showed a beam flexural failure where the plastic hinge formation was at a distance of approximately 250 mm from the beam-column interface. This specimen achieved an increase of 140 % in the load capacity compared to the control specimen.

Azarm et al. in 2017 investigated the ability of CFRP overlays to improve the seismic capacity of RC joints. Two identical specimens of exterior RC joints were fabricated and tested under monotonic load. One of the specimens was considered as a control while the other specimen was retrofitted with the CFRP flange bonded scheme. The retrofitting scheme consisted of five layers (300 mm length) of CFRP laminates were placed on the top and bottom flanges of the beam ends joining the joint and were extended so that they covered parts of the adjoining column faces. 150 mm wide strips with 5 layers of overlay are sufficient to provide the appropriate anchorage for the CFRP sheets. The results showed that the load capacity of the retrofitted joint increased by 23 % compared to the control specimen. Also, relocation of the plastic hinge towards the end of the wrap did not occur where flexural cracks were formed at the face of the column as shown in Figure 2.4 .To investigate the effect of FRP overlay thickness on possible relocation of the plastic hinge in this joint, a numerical investigation was carried out in which three different overlay thicknesses of 5, 7 and 9 layers of overlay, corresponding to thicknesses, respectively. Numerically 9 layers succeed to relocate the plastic hinge place.

An experimental study was conducted by **Mostofinejad** and **Akhlaghi** in 2017 to investigate the seismic behavior of exterior RC beam - column strengthened with CFRP sheets externally bonded reinforcement on grooves (EBROG) and the performance of FRP fans to prevent the splitting

failure of the concrete cover. Six RC specimens without transverse reinforcement in the joint region were constructed and subjected to quasi static reverse cyclic load. On specimen was set as a control while the other specimens were strengthening U and X shaped configurations of CFRP sheets as shown in Figure 2.5 . The results showed the average maximum positive and negative loading directions increased by up to 36, 52, and 17 % for specimens of U-shaped configuration with FRP fan and the specimen with X configuration, respectively, the ductility was enhanced by 74 % and the energy dissipation improved twice compared to the reference specimen. Also, The U-shaped CFRP jackets bonded according to the proposed method are capable of effectively relocating the plastic hinge away from the column interface into the end of the CFRP layers as shown in Figure 2.6 .

(a) Control specimen (b) Retrofitted specimens

Figure 2.4 Crack pattern for retrofitted joints (Azarm et al., 2017)

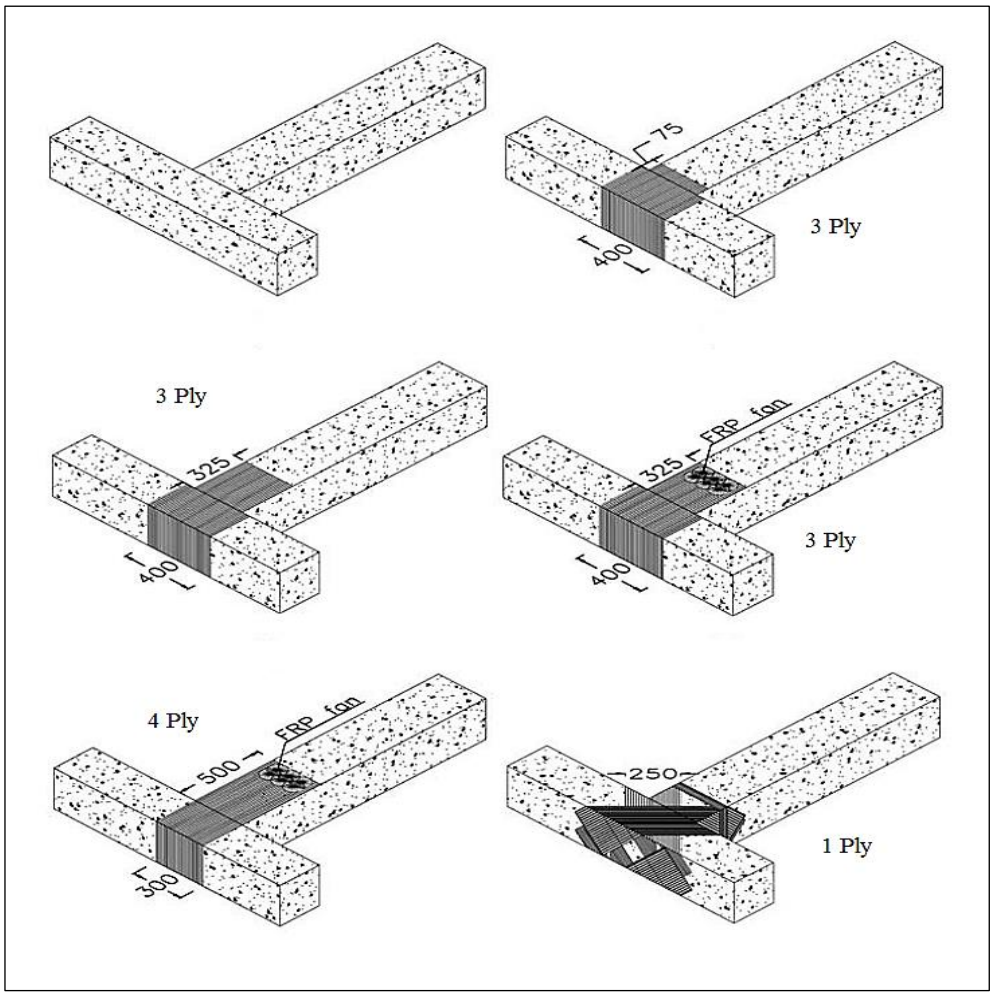

Figure 2.5 Strengthening configurations of the tested specimens (Mostofinejad & Akhlaghi, 2017)

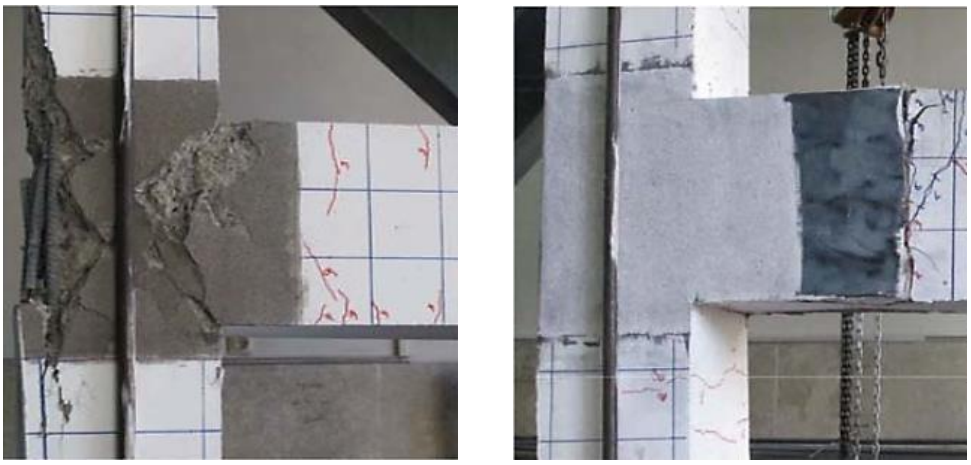

(a) control specimen (b) Strengthening specimen

Figure 2.6 Final failure patterns of the tested specimens (Mostofinejad & Akhlaghi, 2017)

Akash and **Jayasree** in 2018 studied the efficiency of exterior reinforced concrete beam column joint retrofitted using GFRP as externally bonded sheets and NSM strips in different angle (30,45 and 60) degree subjected to reverse cyclic load. The parameters that had been evaluated at this study were stiffness, ductility, energy dissipation and the strength. Ten specimens of exterior joints were casted and tested in this study. The reverse cyclic load was applied to the specimens in two stages (forward and reverse) load. So, the specimens were divided into two identical groups. Each group consisted of five specimens. One of these specimens represented the control specimen, three of them explained the NSM strengthening at the above-mentioned angles while the last one was for the exterior bonded GFRP sheets. The forward (cyclic) load included the same number and details of the specimens mentioned above. Except the control, all the specimens were subjected to preloading up to 67% of the ultimate load of the control. After then the retrofitting was applied to them. All the parameters that were investigated at this study for all NSM retrofitted specimens were more than the control and externally bonded specimens. Moreover, the NSM technique with angle at 30 degree quit proved all the parameters included in this study.

Lin Wang et al. in 2019 experimentally studied the strengthening of seismically deficient RC joints using CFRP. Six exterior RC beam - column joint specimens were subject to cyclic load. These six specimens consisted of one non-seismically specimen, one seismically specimen and four retrofitted specimens using different schemes of bonded CFRP sheets and near surface mounted (NSM) CFRP strips as shown in Figure 2.7 . The concluded result showed that the specimen without any transverse reinforcement in the joint region failed in shear when subjected to cyclic loading while the specimen with shear stirrups appeared flexural failure. Also, using of NSM CFRP composite strips to strengthen an exterior RC

beam - column joint with anchorage of the CFRP composite strips in the adjacent beam was found to be the most effective among the three strengthening schemes examined. The method can effectively relocate the plastic hinge away from the column face, leading to a ductile failure mode as shown in Figure 2.8 .

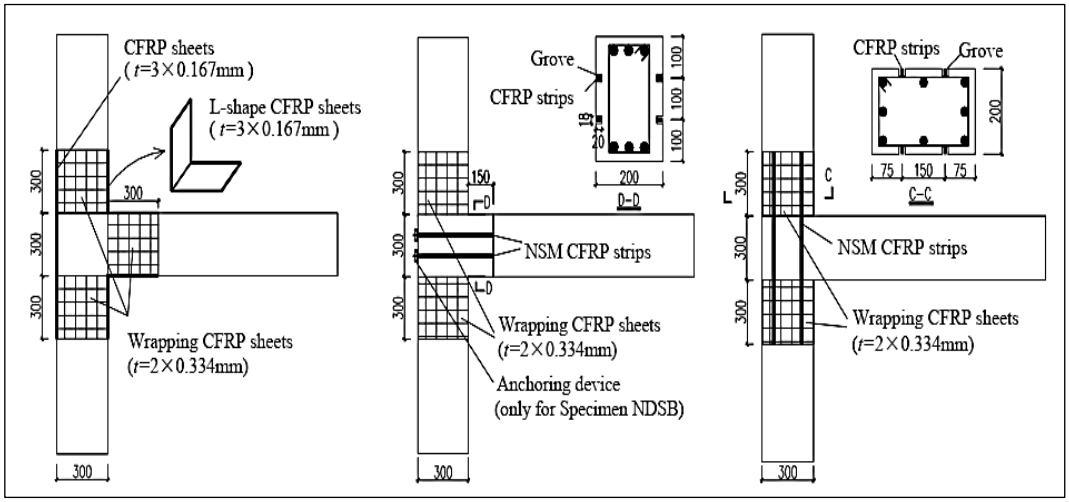

Figure 2.7 Strengthening schemes of tested specimens (Wang et al., 2019)

(a) Non-seismic control specimen (b) Retrofitted specimen

Figure 2.8 Failure modes of tested specimens (Wang et al., 2019)

Arowojolu et al. in 2019 studied the use of CFRP for strengthening reinforced concrete beam - column joint to relocate the plastic hinge location. The test was done on eight specimens of non - seismically externally corner

reinforced concrete joint. They were divided into two sets each contained four specimens. The first set was subject to monotonic load while the second set was subject to cyclic load. One specimen represented the control and the remaining three specimens were the retrofitted specimens by CFRP strip and sheets. One retrofitting scheme was adopted for all retrofitted specimens as shown in Figure 2.9 . The scheme differs in length, thickness and location of the CFRP. One of the two sets subject to monotonic load with scheme length 200, 200 and 300 mm while the other set subject to cyclic load with scheme length 300, 200 and 200 mm. The results of the practical part have been confirmed by using FEM. The results showed that plastic hinge location moved to the end of the CFRP sheet. Also, that required length of the bonded CFRP sheet was lesser than that of the beam depth. The specimens with 200 mm length of CFRP sheet performed better compared to the 300 mm length. The increase of the load capacity was (18.6 and 17.9) % for the retrofitted specimens with bonded CFRP sheet length 200 and 300 mm, respectively under monotonic load while this increase was (24.1 and 10.3) % under the cyclic load.

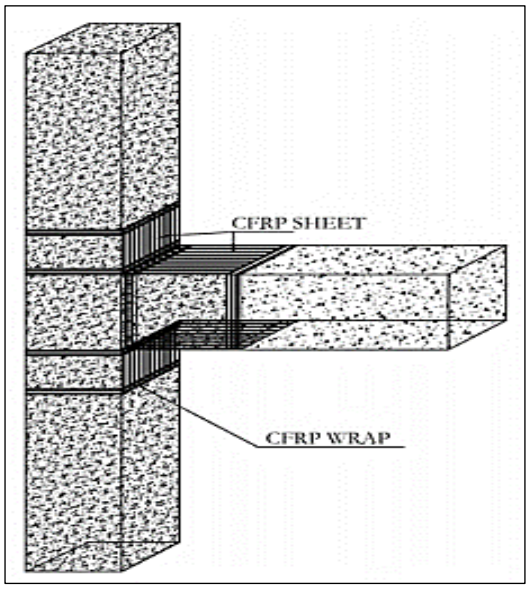

Figure 2.9 Retrofitting scheme of specimens (Arowojolu et al., 2019)

2.2.1.2 Reinforced Concrete Jacketing

Bindhu et al. in 2016 investigated the improvement of the seismic capacity for exterior beam - column joints by using concrete jacketing with newly proposed reinforcement detailing. The newly proposed reinforcement for jacketing consists of additional collar stirrups around the beam–column joint as shown in Figure 2.10 . The specimens were divided into five kinds, the first one represented the non-ductile joint included three specimens that were designated as the control. The second represented the retrofitted specimen using conventional concrete jacketing (without collar stirrups) while the third kind represented the retrofitted specimen using newly proposed jacketing. Two specimens were strengthened using conventional and newly proposed jacketing to represent the fourth and fifth kinds respectively. The concrete jacketing for the last two kinds was casted monolithically with the joint body. All the specimens were subjected to reverse cyclic loading. Each specimen was first loaded up with semi static loading rate 1.962 kN and then unloaded, till Reload was applied on the reverse direction with same loading rate. The subsequent cycles were also loaded in a similar way. The results showed that concrete jacketing changed the failure mode i.e (plastic hinge formation). Also, the specimen with newly suggested jacketing that was casted monolithically was achieved an increase in the load carrying capacity, energy dissipation and ductility by (90, 164 and 36%), respectively compared to the control specimen.

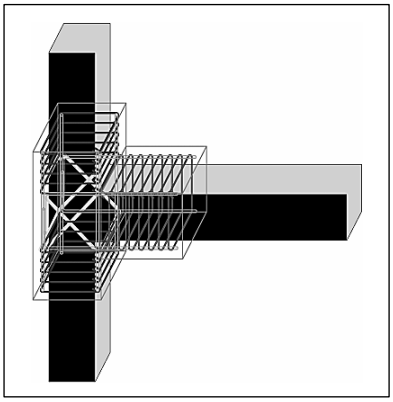

Figure 2.10 Proposed jacketing detail (Bindhu et al., 2016)

2.2.1.3 Ferrocement Jacketing

Kannan et al. in 2013 adopted a ferrocement jacketing as a strengthening technique for exterior reinforced concrete joint subject to cyclic loading. At this study, two kinds of ferrocement jacketing schemes were adopted. The first one was the common kind that was with right angles and designated as conventional jacketing while the second kind of ferrocement jacketing was the advanced jacketing in which the corners of beam and column were filleted almost 20 mm radius before applying the jacketing. The test was conducted on six specimens of the reinforced concrete joint without stirrups at the joint core area. The concluded results explained that using the two jacketing methods enhanced the load capacity by 33.33 % compared to the control specimen. However, the advanced ferrocement jacketing is better than the conventional jacketing where the increase of energy dissipation and maximum deflection was (350.3 and 90.1) % for the specimens with conventional jacketing and (501.1 and 140.8) % for the specimen with advanced jacketing, respectively.

Bansal et al. in 2016 studied the strength behavior of retrofitted RC beam-column joint by using ferrocement jacketing. The test was conducted on five specimens of exterior RC joint with concrete grade M20. The first specimen was subject to monotonic load up to failure and considered as a control while the remaining four specimens were loaded up to 80% the ultimate load. Two retrofitting schemes of 20 mm thick ferrocement jacketing were applied to them, each scheme was applied to two specimens as shown in Figure 2.11 . Then, the specimens were loaded again with similar procedure. The results showed an improvement in the load capacity of retrofitted specimens for both first and second retrofitting schemes increased as compared to control specimen by (27 and 59) %, respectively as well as

to the yield load. Also, there was no noticeable increase in the ductility index where the increase was (9 and 8) % for first and second scheme, respectively.

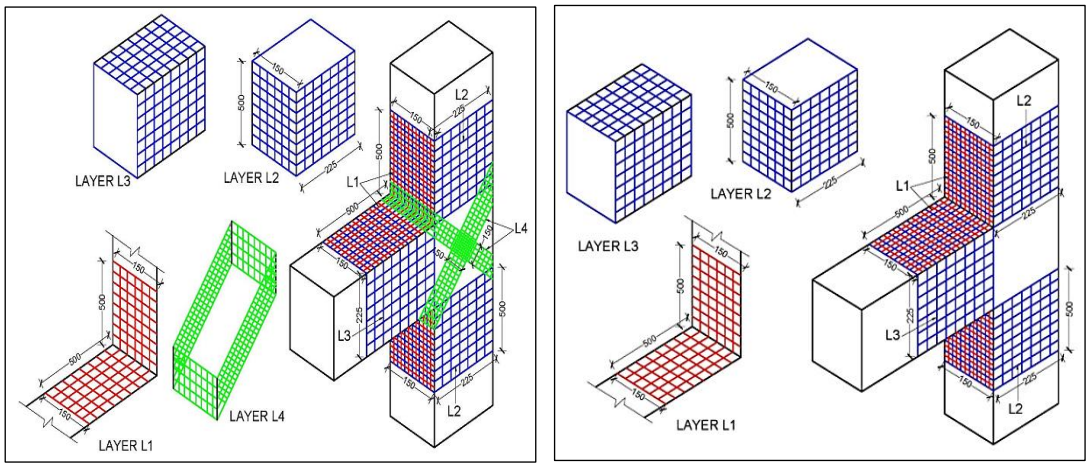

(a) Retrofitting Scheme 1 (b) Retrofitting Scheme2

Figure 2.11 Retrofitting schemes of tested specimens (Bansal et al., 2016)

2.2.2 Strengthening Using Steel plate

Sharbatdar et al. in 2012 investigated the behavior of retrofitted RC exterior beam - column joint by using steel prop and curb (suggested technique). Four half - scale RC joints were tested under the cyclic loading. Two control specimens with the different beam heights were loaded up to their ultimate strength and this was followed by retrofitting of these damaged specimens as new specimens and tested again under the same loading system as shown in Figure 2.12 . Experimental results showed that the 25% reduction of beam height caused decreasing in the ductility, load capacity and energy absorption. The ultimate load for the retrofitted specimens was increased up to 80% and also the energy absorption was enhanced to 93 and 250 % compared to the control specimens with beam of (reduced and normal height), respectively. The cracks were minimized due to a new lateral loading in the beam - column joint region in this upgrading method. Suggested two - side steel prop and curb retrofitting system was usable for rehabilitation the joint specimens because the shear stresses and the number

of cracks at the panel zone were reduced and the plastic hinge was effectively relocated to the above beam curb from side of joint and panel zone in this proposed system as shown in Figure 2.13.

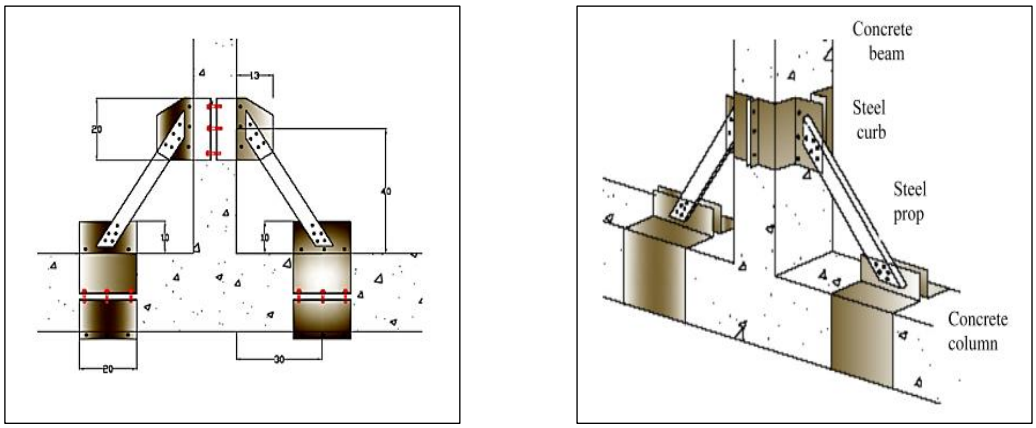

Figure 2.12 Schematic view of retrofitted concrete joints specimens (Sharbatdar et al., 2012)

(a) Control specimen (b) Retrofitted specimens

Figure 2.13 Retrofitted joint specimens at the end of test (Sharbatdar et al., 2012)

Torabi and **Maheri** in 2017 investigated a specimen of exterior RC beam - column joint repaired and retrofitted by using stiffened steel plates. The target of this study was to increase the joint capacity and relocate the plastic hinge location. The cross - sectional area of the original specimen for both beam and column was identical and equal to (300×300) mm^2 while the length of column and beam was (2700 and 1600) mm respectively. Concrete

grade M20 was used for casting the specimen. The specimens were subject to quasi static cyclic load up to failure. After that, the repairing works for the defected specimen was continued until the specimen was fully repaired. Then, the retrofitting works were applied by using 15mm thick stiffened plate that had dimensions, details and the set up clarified in Figure 2.14 . The same load condition was applied to the renovated and retrofitted specimen sample up to failure. This study concluded that using stiffened steel plate to renovate the joint increased the load capacity. The increase was almost 35% for the retrofitted specimen compared to the original specimen. Moreover, the seismic performance of the joint was enhanced by moving the plastic hinge location out of the renovate area.

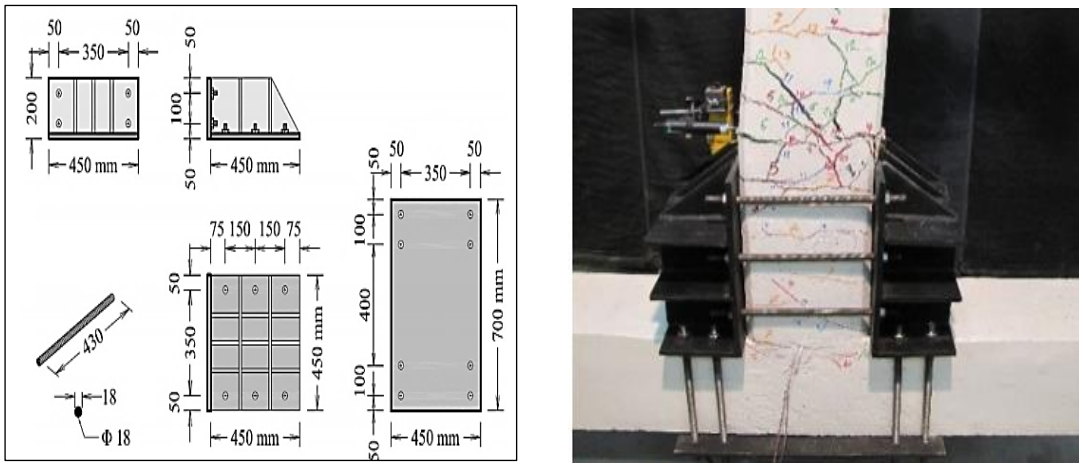

(a) Stiffened Plate Details (b) Stiffened Plate Set Up

Figure 2.14 Stiffened plate detail (Torabi and Maheri, 2017)

2.2.3 Strengthening by Using Steel Fiber Reinforced Concrete

Misir and **Kahraman** in 2013 studied the effect of SIFCON blocks on performance of reinforced concrete beam column joint without seismic reinforcement. The aim of this experimentally study was to use a new strengthening technique for reinforced concrete joint in an existent reinforced concrete frame building. This technique depended on using sheet

and corner block pre-manufactured and fixed at the joint with anchor rod as shown in Figure 2.15 .

The quasi-static cyclic loading test was carried out on three identical specimens in dimensions and reinforcement details. One of them was to serve as a control. While the other were strengthened by plates and corner blocks of SIFCON with different thickness. The test parameters were compressive strength of composite matrix, ratio of fibers, thickness of block and the anchorage length and orientation of the rods. The loading steps were performed at predefined drift ratios starting with (0.15, 0.25, 0.35, 0.50, ..., 3.5) %. As a result, for this study, they succeed to move the location of the plastic hinge away from the face of the column. In other words, the failure mode of this joint changed to be flexural rather than shear failure which considered as a brittle in the control specimen.

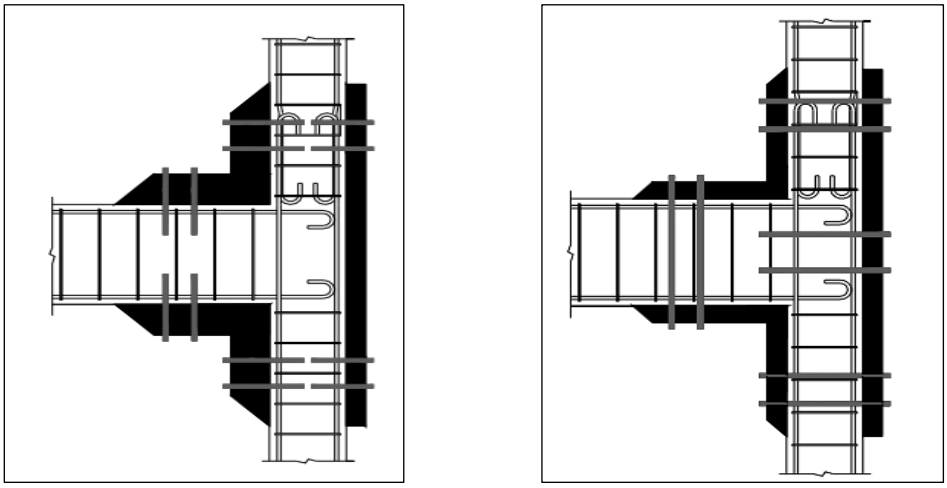

Figure 2.15 SIFCON strengthening (Misir and Kahraman, 2013)

Balaji and **Thirugnanam** in 2017 studied the behavior of exterior reinforce concrete beam - column joint that was improved by SIFCON in the core of that joint under reversed cyclic load. At the experimental part of the study, ten specimens were conducted under five series of test. Two of these specimens were casted with normal concrete strength M30. Four of the

specimens were made of concrete with 1.5 % steel fiber, two of them fully fibrous concrete while the remaining two specimens were made of fibrous concrete in the joint core region. The last four specimens were SIFCON specimens with 9 % steel fiber, two of them fully SIFCON specimens while the remaining two specimens were made SIFCON in the joint core region. Also, FEM was constructed by using ANSYS program to expect the modes of failure and the load deflection relationships of all tested specimens. The results showed that using fibrous concrete led to increase the first cracking load. The predicted load deflection curve from numerical modeling seems to be close to the experimental result. The ultimate load capacity increased by 69 % for the SIFCON joint compared to the normal joint while both SIFCON beam- column joints and specimen with SIFCON in the joint core exhibited a good ductile behavior under the applied load before the final collapse.

Das and **Choudhury** in 2018 experimentally examined the performance of reinforced concrete beam column joint and its performance due to by using different kinds of fiber reinforced concrete. Four identical specimens in dimensions and reinforcement details were casted. The first specimen represented the control while the others three specimens represented three kinds of fibrous concrete. Three kinds of fiber were used in this study with different volume fraction. They were steel, carbon and glass fiber, with volume fraction (0.75, 0.75 and 0.5) %, respectively. The specimens were tested under reverse cyclic load to simulate the seismic effect. The results revealed that the ultimate load for all the specimens containing fibers was more than that of the control specimen. The increase of the maximum load in reverse cycle was 27 % for the specimen of 0.75 % steel fiber.

2.2.4 Strengthening Using Additional Reinforcement Detail

Ha and **Cho** in 2008 achieved an experimental study about using suggested reinforcement details in the strengthening of high strength reinforced concrete joint. The suggested reinforcement details included using of internal closed stirrups for confining concrete and additional intermediate steel bars with hooked ends. The target of this study was to improve the seismic strength and performance of reinforced high-strength concrete exterior joints under cyclic load depending the concept of moving the plastic hinge location away from the face of column. The parameters of this study were the loading type, length of the intermediate steel, the concrete confinement using closed stirrups and the concrete compressive strength. Figure 2.16 shows the tested specimens' details. Advanced reinforcement details were improved the load carrying capacity of reinforced high strength concrete exterior beam - column joints. The location of the plastic hinge moved away from the joint into the beam as shown in Figure 2.17 .

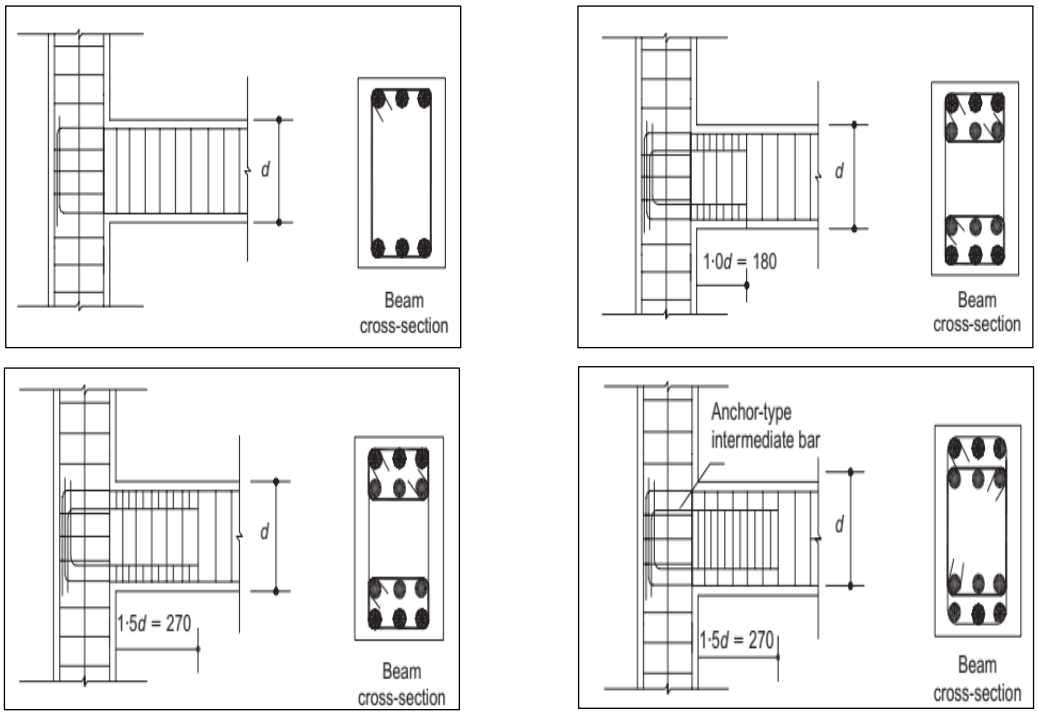

Figure 2.16 Reinforcement details of beam - column joints (Ha and Cho, 2008)

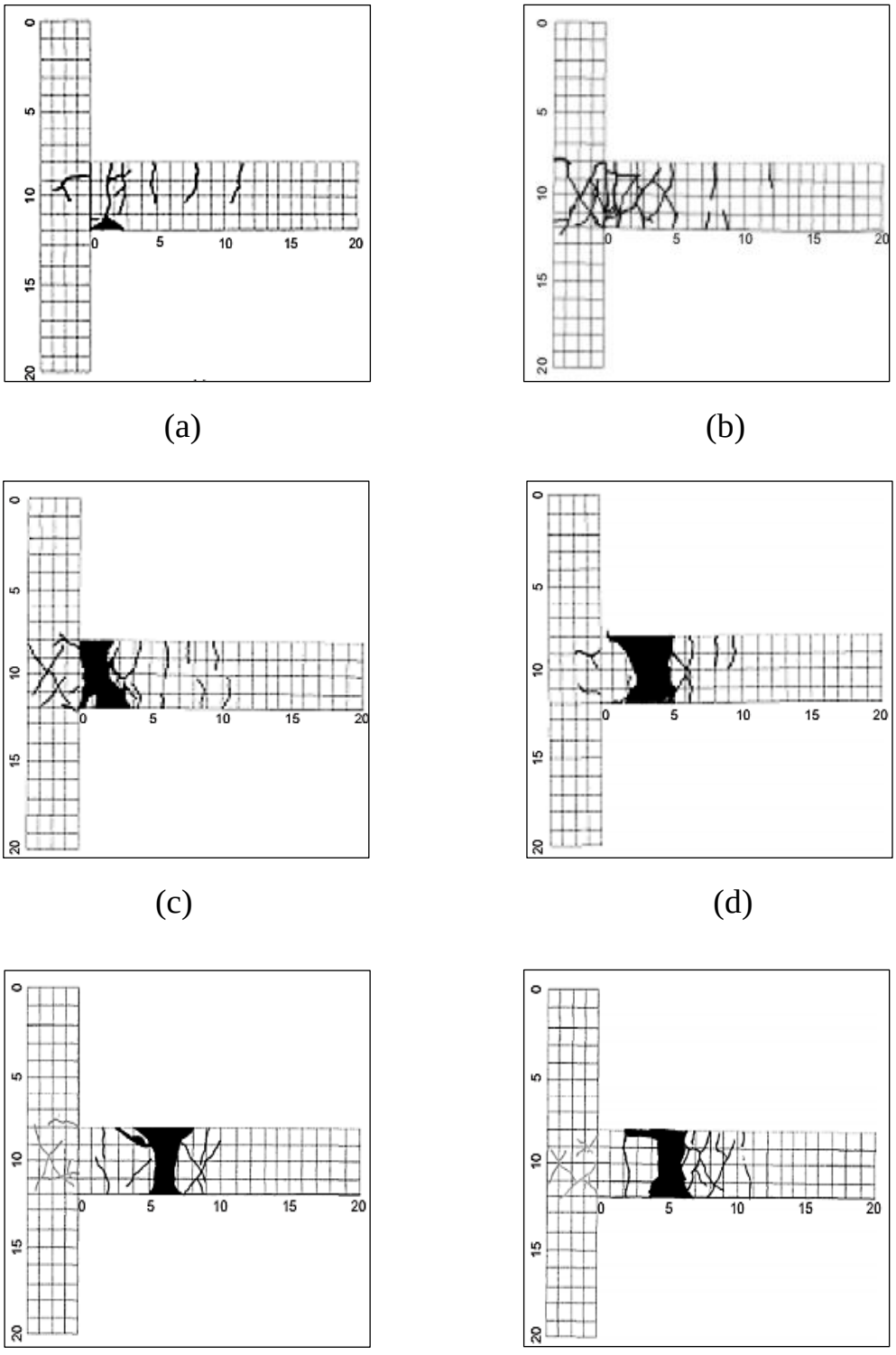

(a) (b)

(c) (d)

(e) (f)

Figure 2.17 The location of plastic hinge at failure (Ha and Cho, 2008)

An experimental study was achieved by **Gokdemir** and **Tankut** in 2017 about exterior reinforced concrete beam - column joint without transverse stirrups at the joint area strengthened using diagonal steel bars. The basic principle of the proposed technique was to implant epoxy anchored bars into the holes drilled through the joint body in the two diagonal directions anchored either by welding or by nuts as shown in Figure 2.18 . The test was done on eleven identical specimens of concrete grade M20. Four of them considered as a reference. Two specimens of the reference had stirrups at the joint region. The number of these stirrups was different depending on the stirrups spacing while the remaining seven specimens were without transverse stirrups at the joint and had been strengthened with diagonal steel bars. The aim of the study was to strengthen the joint to prevent early failure of the joint region prior to hinging in the beam. The variables of the study were the number of stirrups at the joint, anchorage type (without, bolt, or weld), amount of implanted steel and the lap splices.

Figure 2.18 Specimens strengthening (Gokdemir and Tankut, 2017)

For the reference specimens, the results showed the performance of the joint without any ties stirrups at the joint area was very unsatisfactory where both the capacity and behavior improved as the concrete confining at the joint using closed stirrups increased. So, the specimen that had less stirrups'

spacing at the joint achieved acceptable performance. Compared to the specimen without stirrups at the joint, both the ultimate load and ductility were increased by 19 % and 78 %, respectively. For the strengthened specimens corresponding to ultimate load and ductility, the diagonal steel bar implant improved the performance effectively where it represented the required amount of steel placed at the joint with appropriate end anchorages. Both bolted and welded bar ends serve the purpose satisfactorily whereas epoxy embedded implants without any end anchorage are far less effective. The effectiveness of the strengthening was almost directly proportional to the amount of steel embedded. Lap splicing of the implanted diagonal bars appeared to be perfectly acceptable where the results using lap splice approximately closed to that without lap splices.

2.2.5 Strengthening Using Steel Sections

Montava et al. in 2019 achieved an experimental study about strengthening of the reinforced concrete joint by using steel sections placed inside the concrete joint as shown in 2.19 . The aim of this study was to confirm the improvement of the ductile characteristics of steel reinforced concrete joint compared to a conventional RC joint. The work was conducted on six specimens. Two of the six specimens were strengthening by using steel sections (HEB 100 and IPN 140). The other two specimens were strengthened by using a square steel section (140×140×5) mm was filled by concrete individually. Then after hardening, the steel section was embedded inside the specimen to be casted after that. In one of the strengthened specimens with square section, two bars Ø 20 mm were added on both sides. Figure 2.20 shows the cross-section and strengthening of the specimens. The remaining two specimens served as control specimens. The specimens were tested under a vertical load with a cyclic loading-unloading test without any applying load in the opposite direction.

Figure 2.19 Strengthening scheme of the specimens (Montava et al., 2019)

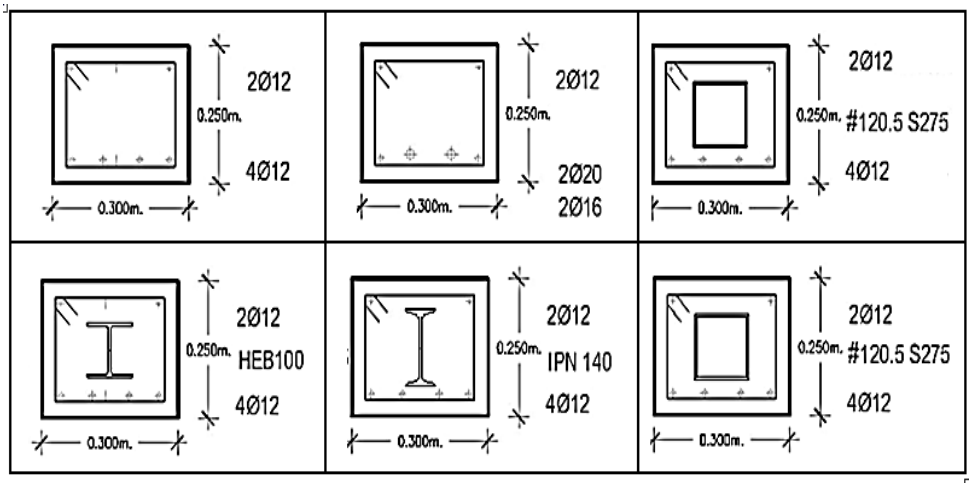

Figure 2.20 Specimens cross-sections and strengthening schemes (Montava et al., 2019)

The results showed that the specimen with embedded square section achieved a maximum load more than the other specimens. Also, the ductility of this specimen increased to be higher than the other. Moreover, the energy absorption of the tested specimens with steel reinforced concrete was greater than that of conventional reinforced concrete specimens.

Montava et al. in 2019 numerically investigated three-dimensional finite element models of reinforced concrete joints strengthened using steel sections to confirm the experimental tests that were carried out on steel

reinforced concrete joints. The aim of this research was to obtain the plastic behavior of reinforced concrete joints with a numerical model in the same way as obtained experimentally. The three specimens were analyzed by numerical simulation using ANSYS program to compare the results with the experimental tests. The model of beam corresponded to a T-joint of a conventional frame with a concentrated load, which corresponded to a horizontal or vertical force as shown in Figure 2.21 Detail of the T- joint in a conventional frame. The load is applied as an imposed displacement in the center of the simply support joint specimen. The obtained results are similar to the results that were obtained from the experimental work.

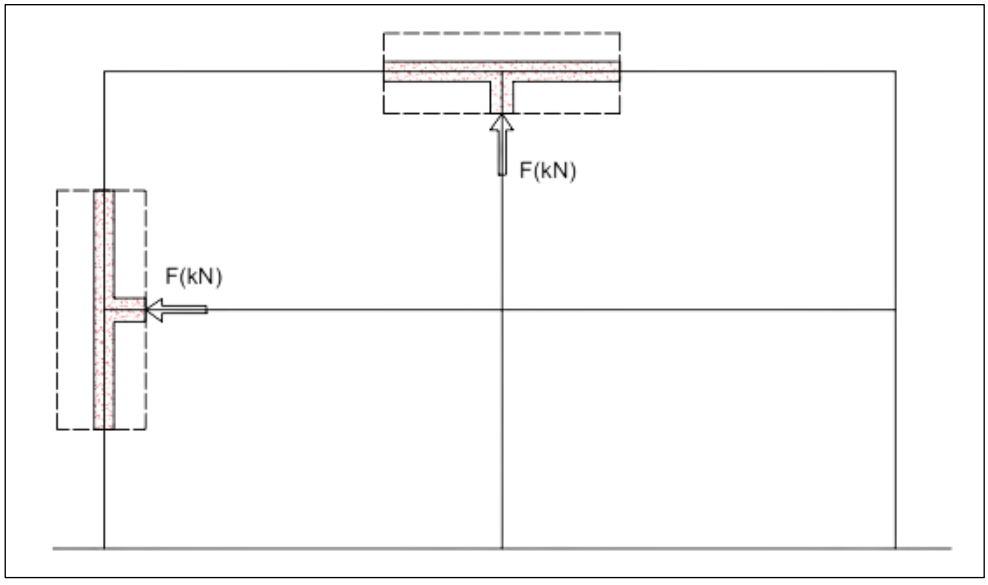

Figure 2.21 Detail of the T- joint in a conventional frame
(Montava et al., 2019)

Abdulghani and **Jaafer** in 2021 numerically studied a nonlinear finite element analysis of RC beam-column joints. A numerical study carried out through a simulation on beam-column joints failed in flexure presented by experimental study. The aim of this study is to analyze beam-column connections under flexural loads simulating the lateral load's condition using the ANSYS program. In this study, the strengthening of the joint was done

using four normal ratios of steel fibers (0.5, 1, 1.5 and 2) % and SIFCON ratios (4, 6 and 8) % with partial and full strengthening cases. The results showed enhancing the ductility and flexural strength of the tested specimens due to the steel fiber. SIFCON concrete enhanced the ultimate strength. The use of steel fibers reinforcement instead of steel rebar enhanced the ultimate load capacity by 101% with large displacement. The full strengthening method by use of SIFCON presented pure flexural failure with cracks spread in the joint region as shown in Figure 2.22

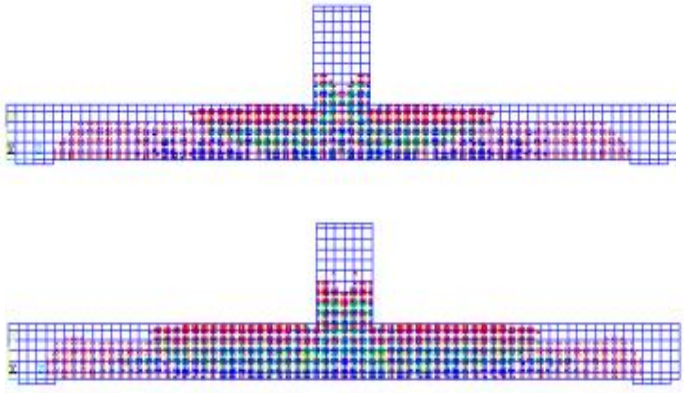

Figure 2.22 Crack pattern and failure modes of RC joint

(Abdulghani and Jaafer 2021)

2.3 Summary

During an earthquake or seismic excitation effect on the reinforced concrete frame buildings, two types of failure can be observed, shear and bond-slip which are considered brittle failures. These affect the overall performance of the joint ductility, load carrying capacity and stuffiness. At the same time many structures have been designed according to the conventional codes without transverse steel at the joint core and that lead sometimes to collapse. To avoid these failures, a lot of studies have been done from which the following conclusions can be drawn:

1. The main aim of many studies was to relocate the location of the plastic hinge formation to be on beam, away from the joint by changing the brittle failure mode to be more ductile.
2. Using composite strengthening techniques in some cases enhance the seismic performance of the RC beam - column joint.
3. The beam - column joint capacity can be improved by confining the concrete at the joint by using closed stirrups.
4. Many studies concerning the improvement of the seismic performance of the RC beam - column joint by using different strengthening techniques. It is clear a few studies were achieved to use steel fiber in strengthening or retrofitting the concrete joint.
5. There is no strengthening or retrofitting of RC joints by using Polyester belts. Therefore, this technique (as the new suggested technique). represents an attempt to investigate the performance of joint strengthening by using a polyester belt.

CHAPTER THREE

EXPERIMENTAL WORK

3.1 General

The main aim of the experimental program is to study the effect of strengthening and rehabilitation of an exterior RC joint by using polyester belt which is a common and economic material as well as the influence of internal reinforcement and concrete compressive strength on the behavior of the joint concerning the ductility, energy dissipation, stiffness, mode of failure and toughness. The specimen's details, methodology of construction, the materials properties, setup and procedure of the test and the tools are showed in this chapter. All the specimens have been prepared and casted then cured for 28 days at the structural materials laboratory of the Civil Engineering Department at Misan University. The casted specimens are transported to the structural materials laboratory of the Technical Institute in Misan province where the strengthening and rehabilitation work with suggested material were applied before testing them there.

3.2 Materials

Many materials were used for casting of concrete mixes for pouring the RC specimens (normal, high and steel fiber reinforced concrete) in addition to the materials used for rehabilitation and strengthening the specimens. These materials are:

Ordinary Portland cement, fine aggregate, coarse aggregate, water, superplasticizer, silica fume, steel fiber, reinforcement steel bars, polyester belt, adhesive materials (Epoxy Sikadur-330, 52LP and 31 CF Slow).

3.2.1 Cement

Ordinary Portland cement type I used for casting all the joint specimens. Its production confirms the Iraqi Standard (I.Q.S) 5/1984. Both physical Characteristics and chemical components of this cement were tested according to the I.Q.S 5/1984 in Al - Karama laboratory and the results are listed in Tables 3.1 and 3.2

Table 3.1 Physical characteristics of cement

Physical property	Test result	Limit of I.Q.S No.5/1984
Fineness (Blain Air permeability Apparatus, (m2/kg)	279	≥ 230
Setting time (Vicat apparatus)		
- Initial (minute)	105	≥ 45
- Final Dilatation angle (hour)	4.25	≤ 10
Soundness (%) (Autoclave expansion)	0.18	≤ 0.8
Compressive strength (MPa)		
3 days	20	≥ 15
7 days	26.5	≥ 23
28 days	33	-

Table 3.2 Chemical characteristics of cement

Chemical analysis	Percent (by Weight)	Limit of I.Q.S No.5/1984
SiO_2	22.30	-
Al_2O_3	4.50	-
Fe_2O_3	3.30	-
Lime Saturation Factor (L.S.F)	0.88	0.66-1.02
MgO	2.15	≤ 5.0
$3CaO.Al_2O_3$ (C_3A)	6.34	-
SO_3	2.35	≤ 2.8
Loss on Ignition (L.O.I)	3.35	≤ 4.0
Insoluble Residue (I.R)	0.98	≤ 1.5

3.2.2 Fine Aggregate

Natural graded sand with modulus of fineness 2.6 was supplied from Al - Basra Province in order to use it in all types of concrete mixes within this research for pouring the specimens. Sieve analysis was carried out on sand sample to check its limits and compare them with the limits of the I.Q.S No. 45/1984 (gradation zone II). The test result conformed to the standard and was listed in Table 3.3. Figure 3.1 shows the gradation of the sand according to the I.Q.S No. 45/1984.

3.2.3 Coarse Aggregate

Crushed gravel of 10 mm maximum size was supplied from north of Misan Province to be use in two types of concrete mixes NSC and HSC for casting samples that consist of these two types of concrete. Before using this aggregate, it must be cleaned and freed of dust. The used gravel was confirmed to the I.Q.S No.45/1984. The test result conducted on a gravel sample was listed in the Table 3.4 and represented in the Figure 3.2

Table 3.3 Sieve analysis result of fine aggregate

Sieve Size	Passing (%)	Limit of I.Q.S No.45/1984 (Zone II)
10 (mm)	100.00	100
4.75 (mm)	96.80	90-100
3.36 (mm)	85.60	75-100
1.18 (mm)	73.60	55-90
600 µ	36.00	35-59
300 µ	17.60	8-30
150 µ	1.40	0-10
Sulfate Content %	0.35	≤ 0.5

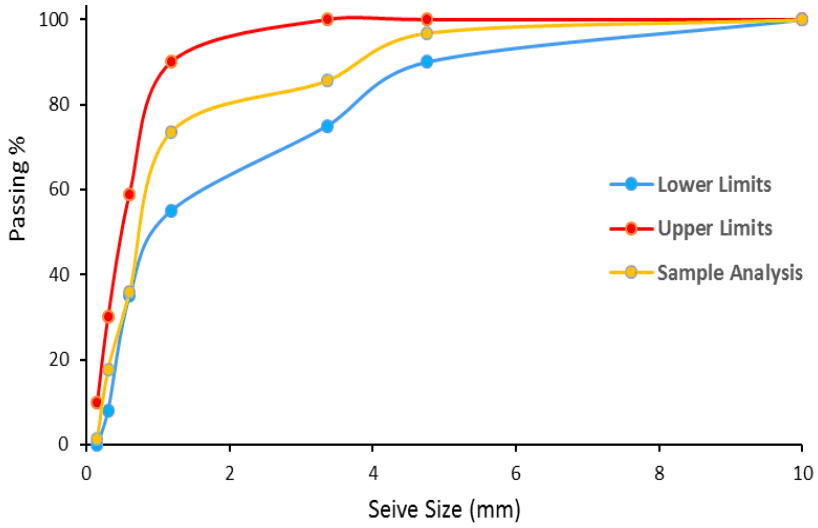

Figure 3.1 Gradation of sand sample

Table 3.4 Sieve analysis result of coarse aggregate

Sieve Size (mm)	Passing (%)	Limit of I.Q.S No.45/1984
14	100	90-100
10	95	85-100
5	8	0-25
2.36	3	0-5

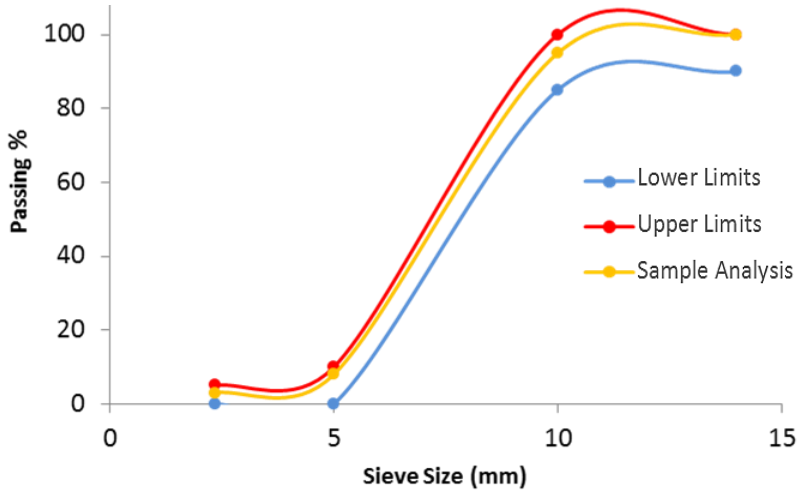

Figure 3.2 Gradation of gravel sample

3.2.4 Water

Reverse osmosis (RO) water as used in all the concrete mixes and curing process. It was added to the concrete mix as a percentage of the weight of the cement or cementitious material (water cement ratio W/C). Water to cement ratio is 50 % for NSC while the water to binder materials (cement and silica fume) is (23 and 19) % for HSC and SFRC, respectively.

3.2.5 Superplasticizer

The water cement ratio affects many characteristics of the concrete mix. So, using a high range water reducer (HRWR) admixture works to improve the fresh concrete properties by reducing the quantity of water added to the mix and increasing the workability. The properties of the concrete mix will be improved by using HRWR such as the concrete compressive strength, density, permeability, the cracks due to shrinkage. In this study, Hyperplast PC260 superplasticizer type was used in HSC and SFRC mixes at proportions (2 and 3) %, respectively by weight of cementations materials (cement + silica fume). Hyperplast PC260 should be added to the concrete with the mixing water to achieve optimum performance. It's met the requirements of ASTM C494/C 494M - 05a (ASTM, 2005). Some characteristics of the superplasticizer PC260 mentioned at the data sheets of the product supplied by the manufacture company listed in the Table 3.5 (DCP, 2019).

3.2.6 Silica Fume

Silica fume is a by-product from the production of elemental silicon or alloys containing silicon in electric arc furnaces. At a temperature of approximately 2000 C^{o} the reduction of high-purity quartz to silicon produces silicon dioxide vapor, which oxidizes and condenses at low

temperatures to produce silica fume. Silica fume particles are spherically shaped and very fine, having a mean size of 0.1- 0.3 µm (Panesar, 2019). The used Silica fume or micro - silica at this study, grey ultra - fine powder produced by DCP company and conform the requirements of the ASTM C 1240-03a (ASTM, 2003) according to the company guides. It was used in both HSC and SFRC mixes with ratios (10 and 22) %, respectively by weight of the cement.

Table 3.5 Hyperplast PC260 technical characteristics (DCP, 2019)

Property	Hyperplast (PC260)
Form	Liquid
Color	Yellowish to brownish liquid
Specific gravity	1.1 + 0.02
Relative density (@ 25 C^{o}	1.08-1.12
Air entrainment	Typically, less than (2%) additional air is entrained above control mix at normal dosages
Dosage	(0.5 - 3.0) liter per 100 kg of cementitious materials in the mix.
Packaging	Available in 25-liter pails, 210-liter drums and 1000 liter bulks.
Storage	between 2° C and 50° C
Standards	ASTM C494

3.2.7 Steel Fiber

Steel fiber is a relatively new construction material. It has been proved as a reliable construction material that has superior performance effects when used in concrete and could improve the characteristics of concrete, compared to the conventional normal concrete in the following properties: higher flexural strength, better tensile strength, higher shock resistance, and crack

resistance (Hassouna & Jung, 2020). Many shapes of steel fibers are available. Straight steel fiber with 14 mm length, 0.2 mm diameter and aspect ratio 70 have been used at this study (see Figure 3.3). It was supplied to the site as bags weight 20 Kg for each to be used for casting the steel fiber reinforced concrete specimens where it represents 2 % by total volume of specimens. It is significant to ensure uniform distribution of steel fibers throughout the concrete mix. Therefore, steel fiber was added equally and gradually during the mixing process.

Figure 3.3 Straight steel fiber

3.2.8 Reinforcement Steel Bars

Deformed mild steel bars conformed to the I.Q.S 2091/1999 are used as reinforcement for the specimens. For the main reinforcement in both beam and column, Ø10 mm bars. Also, Ø6 mm Turkish steel bars were used for the closed shear stirrups and ties. Tensile test was carried out on a sample of these bars at the structural laboratory of Technical Institute of Amarah. Figure 3.4 shows the testing machine and the test results were listed in Table 3.6 and Figure 3.5

Figure 3.4 Testing machine of steel bars

Table 3.6 Steel bars test results

Nominal Diameter (mm)	Actual Diameter (mm)	Stress (MPa)		Elongation %
		Yield (f_y)	Ultimate (f_u)	
6	5.97	442.62	503.6	11.1
10	9.46	560.6	652.5	12.4
Limits of I.Q.S 2091/1999				
6	± 0.5	300	500	11
10		400	600	9

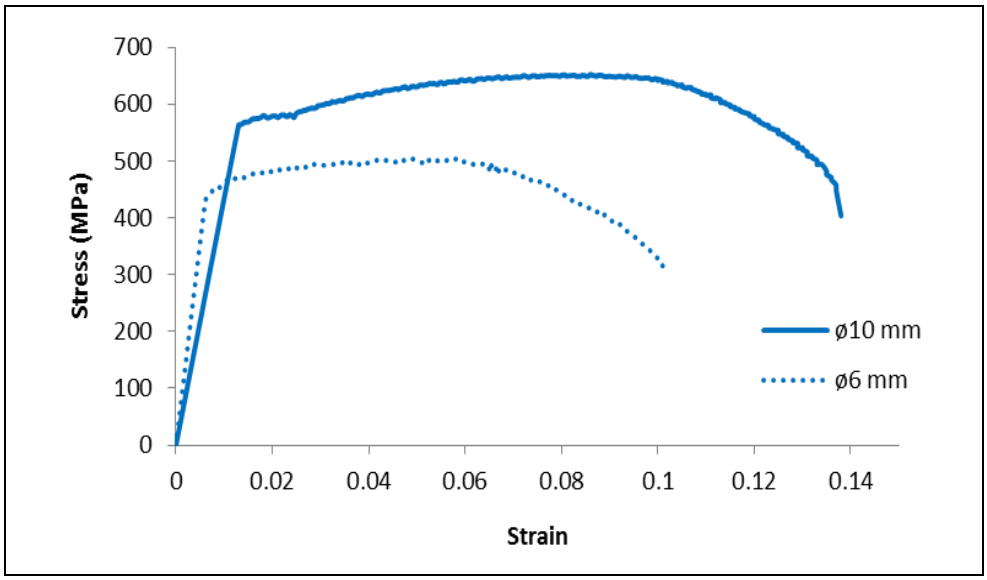

Figure 3.5 Stress - strain curve for tested reinforcement steel bars

3.2.9 Polyester Belt

In this study, a polyester belt was used with epoxy Sikadur - 330 for applying the strengthening and rehabilitation schemes to the RC specimens. It's made from polyester fibers which is considers as a common material due it using for multi purposes in our life and its cheap price in the local markets. This material has been supplied as a roll with 7.5 m length then it cut according to the strengthening scheme dimensions. The polyester belt properties are listed in Table 3.7. Figure 3.6 shows the polyester belt testing.

Table 3.7 Polyester belt properties

Length (mm)/roll	Width (mm)	Thickness (mm)	Test Load (kN)	Ultimate Tensile Stress (MPa) (average of Three Samples)
7500	60	3	52.2	290

Figure 3.6 Polyester belt testing

Figure 3.6: Continued

3.2.10 Adhesive Materials

In this study, three kinds of epoxy produced by Sika company as shown in Figure 3.7 were used. Sikadur - 330 was used for strengthening the specimens as adhesive materials for bonding the polyester belts on the concrete surface. In rehabilitation work, Sikadur - 52 LP used for sealing and filling the cracks and damaged areas of the joint specimens while Sikadur - 31 CF Slow used as a resin to close the cracks and prevent the injected epoxy to pull out under the pressure of injection.

Figure 3.7 Types of adhesive material (epoxy)

3.2.10.1 Epoxy Sikadur - 330

Epoxy Sikadur - 330 was used for fixing the polyester belt to the area which will be strengthened at the surface of concrete specimens. It is available as two components A and B. These components are mixed together using a mix ratio of 4:1 by weight, respectively. The mixing time should continue until the mix be in a uniform grey color. Technical information as provided by the manufacturer was listed in Table 3.8 (Sika, 2020c).

Table 3.8 Technical properties of Sikadur - 330
(Sika, 2020c Product Data sheet).

Property	Description			
Flexural Strength	60.6 N/mm^2 (7 days at +23 °C)			
Modulus of Elasticity in Flexure	3489 N/mm^2 (7 days at +23°C)			
Tensile Strength	33.8 N/mm^2 (7 days at +23 °C)			
Elongation at Break	1.2 % % (7 days at +23 °C)			
Mixing Ratio	Component ‘A’: Component ‘B’ = 4 : 1 by weight			
Pot Life	57 minutes			
Compressive Strength (MPa)		16 °C	23 °C	32 °C
	7 days	80.0	77.2	81.3
	14 days	85.5	81.3	82.0

3.2.10.2 Epoxy Sikadur - 52 LP

Epoxy Sikadur - 52 LP is a liquid resin used for injection and characterized as low viscosity, perfect adhesion for different materials including concrete. Used to fill and closed the cracks in the damaged concrete joint specimens by injecting the epoxy to the specimens under 40 bar pressure using pressure machine. It is available as two parts A and B with mixing ratio 2:1 by weight, respectively. The two components of epoxy should be mixed using electrical drill for at least three minutes at which the mix be in a uniform pale straw color. Technical information provided in a product data sheet as provided by the manufacturer were listed in Table 3.9 (Sika, 2020a).

Table 3.9 Technical properties of Sikadur-52 LP
(Sika, 2020a Product Data sheet).

Property	Description	
Tensile Strength	~ 27 MPa (7 days at 30 °C)	
Substrate Temperature	25 °C min. / 40 °C max.	
Mixing Ratio	A : B = 2 : 1 parts by weight	
Pot Life	Temperature	1kg Mixture
	5 °C	-
	10 °C	-
	23 °C	~ 70 minutes
	30 °C	~ 30 minutes
	40 °C	~ 10 minutes
Tensile Adhesion Strength	Curing Time	Curing Temperature 25°C
	2days	≥ 7 MPa
	14days	≥ 10 MPa
Compressive Strength	≥ 70 MPa (7 days at 30 °C)	

3.2.10.3 Epoxy Sikadur - 31 CF Slow

Sikadur - 31 CF Slow can be used as mortar and adhesive material. It can be used for several construction and repair works. It is available as two parts A and B with mixing ratio 2: 1 by weight, respectively. At this study we used it to close the big crack and damage area before injecting Sikadur - 52 LP to satisfy a confining to insure completely filling with epoxy resin for all cracks. Technical information provided in product data as provided by the manufacturer were listed in Table 3.10 (Sika, 2020b).

Table 3.10 Technical properties of Sikadur - 31 CF Slow (Sika, 2020b Product Data sheet).

Property	Description	
Tensile Strength	(20-25) MPa after 10 days at (20-30) °C	
Modulus of Elasticity in Tension	4300 MPa	
Shear Strength	Bond strength to concrete	(15-20) MPa after 10 days at (20-30) °C
	Bond strength to steel	(3-3.5) MPa after 10 days at (20-30) °C
Mixing Ratio	Component A : component B = 2 : 1 by weight	
Pot Life	Temperature	1kg Mixture
	5 °C	-
	10 °C	-
	20 °C	90 minutes
	30 °C	50 minutes
	40 °C	25 minutes

3.3 Mixing procedure for concrete

Electrical mixer was utilized for mixing concrete used in this study. Two mixers were used, horizontal rotary and drum mixer type with capacity (0.08 and 0.24) m^3, respectively. The horizontal mixer of 0.08 m^3 capacity

was used for producing SFRC mixes while the drum mixer of 0.24 m^3 was used for producing both NSC and HSC mixes. Figure 3.8 shows the two mixers used in this study. The mixing procedure of NSC and HSC samples was implemented by adding coarse aggregate followed by fine aggregate and mix them together for one minute. The cement or cementitious materials (cement and silica fume) were added and mixed with aggregate to ensure homogenous mixing for the materials. After that, the water and superplasticizer added, respectively. In SFRC, the procedure was carried out by adding fine aggregate and half of the water amount firstly followed by cementitious materials and mixed them for two minutes until the mix was homogeneous. Then, steel fiber by 2 % of mix volume was added gradually and mixed with pervious materials for five minutes to achieve homogenous distribution for all ingredients. At last, the remaining water amount and superplasticizer were mixed together then added to the mix. All the materials mixed together for forty minutes to satisfy good workability for concrete. The water ratio was 50 % by weight of cement for NSC while for HSC and SFRC it was 23 % and 19 % by weight of binder materials, respectively. Table 3.11 shows the quantities of the used materials for each type of concrete per cubic meter.

(a) Horizontal Rotary Mixer (a) Drum Mixer

Figure 3.8 Concrete mixers types

3.4 Specimens Details

The experimental study of this research was done on fifteen RC joint specimens. These specimens divided into three groups according to the concrete type. The first group "A" included ten specimens fabricated using NSC. Three specimens were included in the second group "B" of HSC while the third group "C" consisted of two specimens of SFRC. All the specimens were identical in dimensions.

Square column with 170 mm cross sectional dimensions and 400 mm length jointed to a rectangular beam with (170 x 200) mm cross sectional and 2400 mm length. Three reinforcement details were adopted for reinforcing the specimens. Conventional or normal reinforcement detail D1 consists of 2Ø10 mm top and bottom as a longitudinal reinforcement beam and 4Ø10 mm in column. Ø6 mm as closed shear stirrups for beam distributed at 140 mm distance along the beam length as well as Ø6 mm spaced at distance 120 mm as ties for column. The second reinforcement detail D2 2Ø10 mm top and bottom as a longitudinal reinforcement beam and 4Ø10 mm in column. Ø6 mm spaced at distance (120 and 140) mm in column and beam as ties and stirrups, respectively. Additional internal reinforcement, 2Ø10 mm top and bottom as a longitudinal reinforcement along the middle third of the beam surrounded by closed stirrup Ø6 mm spaced at140 mm. Moreover, additional main reinforcement 2Ø10 mm and Ø6 mm hooks spaced at 120 mm for the column. The third detail D3 was as of the D2 reinforcement detail except the additional longitudinal reinforcement along the middle third of the beam surrounded by double closed stirrups. Figure 3.9 and Table 3.12 display the details of joint specimens.

Table 3.11 Quantities of concrete mix materials (per cubic meter)

Materials	Concrete Type		
	NSC	HSC	SFRC
Cement (kg/m^3)	450	500	950
Fine aggregate (kg/m^3)	562	625	1050
Coarse Aggregate (kg/m^3)	675	750	-
Silica fume (kg/m^3)	-	50	209
Water (L/m^3)	225	125	220
Steel Fiber (kg/m^3)	-	-	156
Hyperplast PC260 (kg/m^3)	-	11	34.77

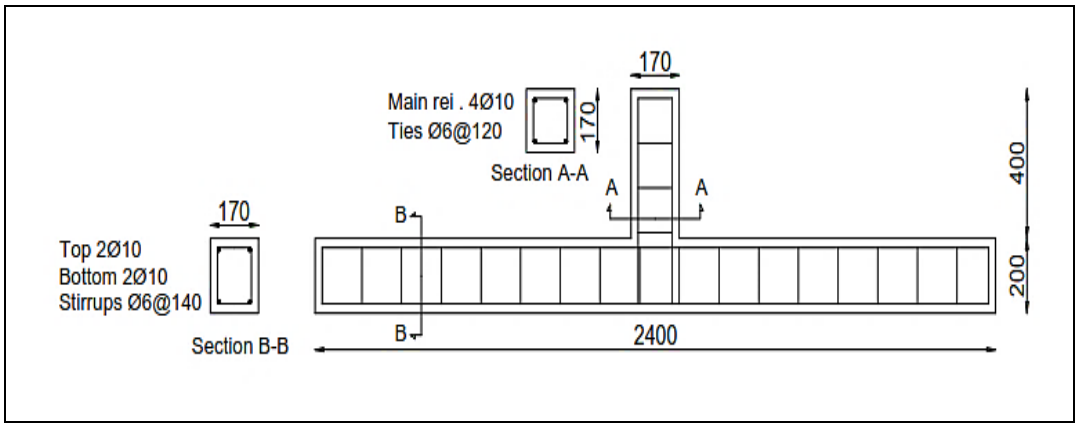

(a) Reinforcement detail (D1)

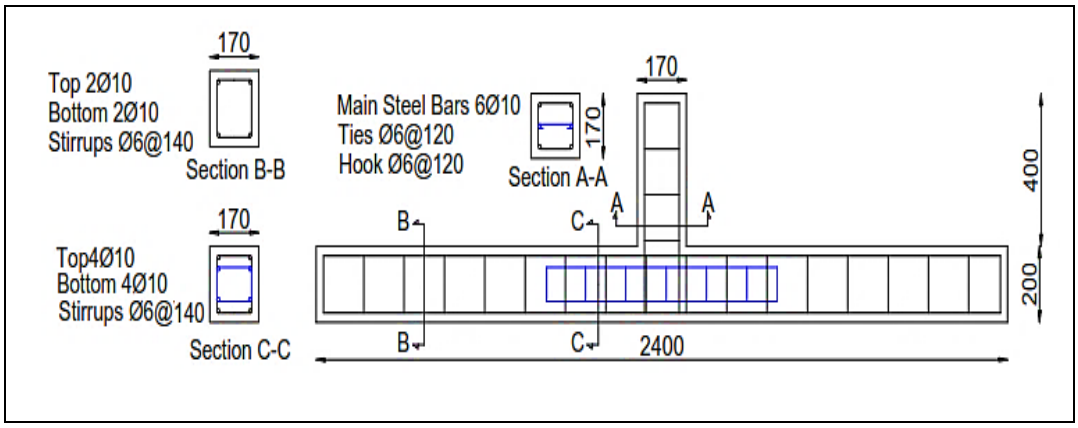

(b) Reinforcement detail (D2)

Figure 3.9 Beam - column joint specimens' details

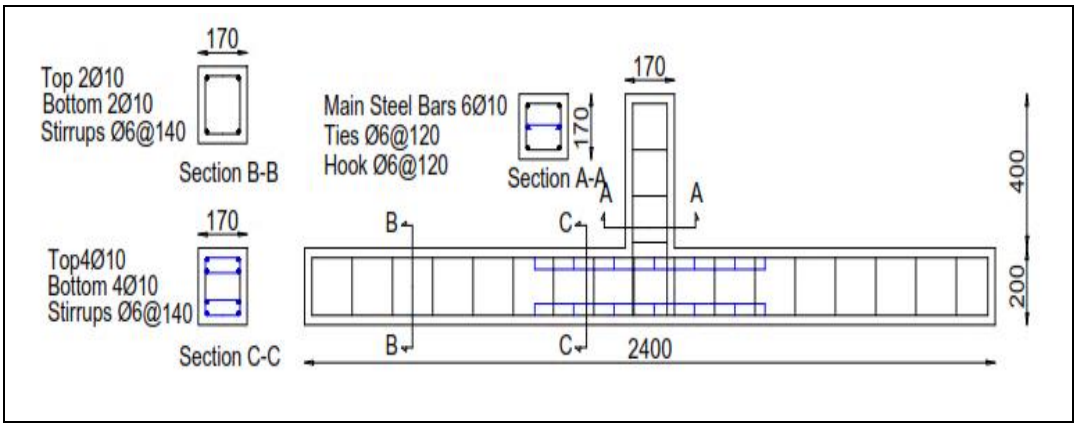

(c) Reinforcement detail (D3)

Figure 3.9: Continued

Table 3.12 Beam - column joint specimens details

No.	Designation	Description	Reinforcement Details	Concrete type	Group
1	C1	Control	D1	NSC	A
2	C2				
3	N1D2		D2		
4	N2D3		D3		
5	H1D1	Control	D1	HSC	B
6	H2D2		D2		
7	H3D3		D3		
8	F1D1	Control	D1	SFRC	C
9	F2D2		D2		
10	S1U	Strengthening	D1	NSC	A
11	S2UL				
12	R1UL	Rehabilitation 70% damage	D1	NSC	A
13	R2L2				
14	R3L2	Rehabilitation 100% damage	D1	NSC	A
15	R4UL				

3.4.1 Specimens Designations Details

All the letters and numbers in the specimens' designation have a specific indication refer to the following:

The first letter to the left, the letter C which refers to the word "Control". For the next five specimens, the first letters of their designation N and H refer to the concrete types (Normal and High) strength, respectively while the letter F refers to the word "Fiber", which indicates using of steel fiber in its producing, which represents steel fiber reinforced concrete (SFRC). The letters (S and R) refer to words (Strengthening and Retrofitting), respectively. The first number to the left, represents the sequence of the specimens. The letter D and the number following it from the right indicate details of the reinforcement D1, D2 and D3. The letters (U and L) that were included in the strengthened and retrofitted specimens refer to the schemes of the strengthening or rehabilitation. The letter (U) indicates the U-shaped scheme while the letter L refers to the word "Longitudinal" that means strips attached to the base of the beam. If the two letters exist together, that means using two schemes for strengthening or rehabilitation. The number following the letter (L) in the specimen designation refers to the layers of longitudinal scheme.

3.5 Casting RC Specimens

3.5.1 Wooden Molds preparation

Thirteen wooden molds (T- shaped) with same dimensions have been fabricated at the carpentry workshop. The mold had a column with square cross section (170×170) mm and beam with rectangular cross section (200×170) mm. The length of the column and beam were (400 and 2400) mm, respectively. Plywood sheets 20 mm thick were cut mechanically to ensure soft and straight edges making right angles when

connected together using nails and screws. After that, these molds were transported to the laboratory to be ready for reinforcement work.

3.5.2 Specimens Reinforcement

Preparation of the steel cages for the specimen was done according to the specific dimensions and reinforcement details. The wooden molds were lubricated and distributed at the casting site correctly to ensure smooth movement during the casting process. After that, the steel cages were placed at the molds to be ready for casting the concrete as shown in Figure 3.10 .

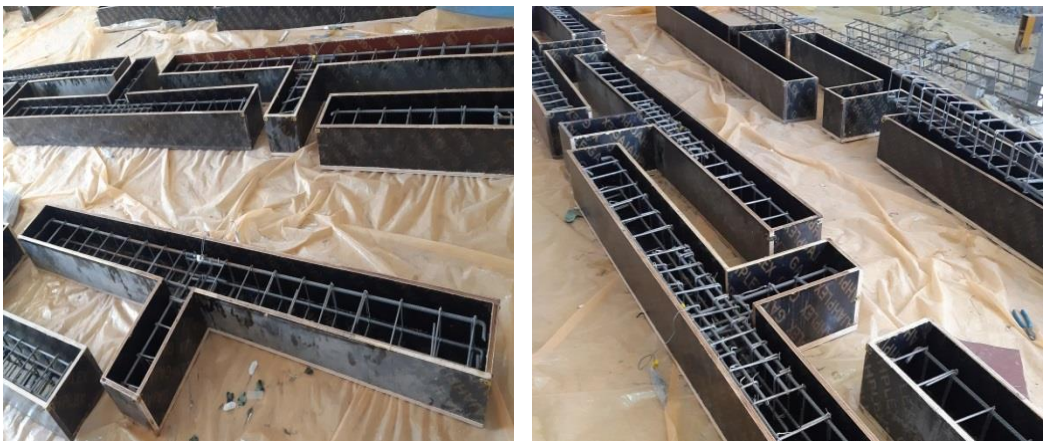

Figure 3.10 Reinforcement the specimens

3.5.3 Concrete Pouring

All the materials used for casting the specimens were weighted and stacked in a clean and dry place before the mixing process. Electrical concrete mixers were adopted for pouring the specimens. The materials were added to the concrete mixer sequencely according to the specified quantities and mixing procedure for each type of concrete. Then, the fresh concrete was poured in each wooden mold in two layers. The compaction was done to each concrete layer using electrical vibrator. Finally, the fresh concrete was levelled manually by using a trowel. After two days, when the concrete started to be hard, the wooden molds were removed and the curing process

continued for 28 days. All the RC specimens were covered by using nylon sheets to. Figure 3.11 shows casting and curing of the specimens. After 28 days which is the end of the curing period, the RC specimens were transported to the laboratory of the Technical Institute of Amarah to be ready for test and application the strengthening and retrofitting schemes using polyester belt.

Figure 3.11 Casting and curing the specimens

3.6 Strengthening and Retrofitting RC Specimens

The strengthening and retrofitting techniques were applied to normal concrete specimens with reinforcement detail D1. The steps of each of them and their schemes will be explained later. Table 3.13 presents the strengthening and retrofitting schemes detail.

Table 3.13 Strengthening and retrofitting details

Specimen	Description	Beam	No. of Layer	Column	No. of Layer
S1U	Strengthening	U shape	1	Wrapping	1
S2UL	Strengthening	U shape	1	Wrapping	1
		Longitudinal	1		
R1UL	Retrofitting	U shape	1	Wrapping	1
		Longitudinal	1		
		Additional 2 Strips wrapping at the Face of Column both sides.	1		
R2L2	Retrofitting	Longitudinal	2	Wrapping	1
		Additional 2 Strips wrapping at the Face of Column both sides.	1		
R3L2	Retrofitting	Longitudinal	2	Wrapping	1
		Additional 2 Strips wrapping at the Face of Column both sides.	1		
R4UL	Retrofitting	U shape	1	Wrapping	1
		Longitudinal	1		
		Additional 2 Strips wrapping at the Face of Column both sides.	1		

3.6.1 Strengthening of RC specimens

Two strengthening schemes were applied on two new construction RC beam - column joint specimens using polyester belt (new technique). The firs scheme was applied to the specimen S1U that included wrapping for the column and only (U-shaped) strengthening for the beam while the other scheme was applied to the specimen S2UL that consisted of wrapping for the column. A single layer of polyester belt was put along the bottom soft of the

beam in longitudinal direction. Also, a layer of U-shape of polyester belt was placed around the beam to cover the soft and lateral sides of the beam. Figure 3.12 shows the strengthening schemes. Before application the strengthening materials to the RC specimens, the following steps were achieved:

1. Roughening the surface of the specimen by using electrical grinder to increase the friction between the surface and the strengthening materials.
2. Cleaning the surface by using air blower to remove any suspended dust. After that, washing the specimen using clean water and then left to dry for one day.
3. A layer of primer epoxy (hardener and base) with 1:4 mix ratio was applied to the concrete surface by using brush. After that, very fine sand with maximum aggregate size (0.3 - 0.6) mm was sprayed on the primer layer to enhance the surface friction.
4. At last, the polyester belt was cut according to the specific dimension of the strengthening scheme. Epoxy Sikadur®-330 (base and hardener) with (4:1) mix ratio were mixed and applied to the concrete surface. Layer of polyester belt was applied to the prepared area then pressed manually using steel roller to remove the air under the belt. Figure 3.13 briefs the strengthening steps.

3.6.2 Retrofitting RC specimens

Four damaged RC beam column joint specimens with reinforcement detail D1 were retrofitted by using polyester belt. These specimens were tested firstly under monotonic load up to (70 and 100) % of their ultimate load. The first two specimens R1UL and R2L2 were tested up to 70 % of the average ultimate load of the control specimens, then the retrofitting process was done to them. The other two specimens are C1 and C2, after testing them

to fully damage 100% of the ultimate load. The retrofitting schemes were applied to them. They were designated as R4UL and R3L2, respectively. Two retrofitting schemes were adopted. The first one was applied to the specimens R1UL and R4UL, which included wrapping the column, single longitudinal layer of polyester belt was soft to the base of beam to cover all the base area followed by U shape layer applied to the beam to cover its base and the parallel two sides. Then, additional two strips were put on the beam adjacent the faces of column perpendicular to the beam with width equal to 200 mm. The second scheme was applied to the specimens R2L2 and R3L2. Its consisted of wrapping the column, two longitudinal layers soft to the base of beam to cover all the base area and additional two Strips wrapping the beam adjacent the faces of column perpendicular to the beam. Figure 3.14 shows retrofitting schemes.

Before applying the Retrofitting to the RC damaged specimens, many steps were performed:

1. Preparing the damaged specimens that were tested by cleaning and remove all loose concrete from the damaged area and cracks.
2. Installing the injection needles and packers at the racked that will inject after drilling small holes along the crack path.
3. Sealing the cracks and the area around the injection needles and packers using paste of epoxy Sikadur®- 31 CF Slow two parts (base and hardener) with mixing ratio 2: 1, by weight respectively to prevent the epoxy from leaking out. The specimens left one day, then low viscosity resin epoxy Sikadur®52 LP two parts A and B with mixing ratio 2:1 by weight was injected into the cracks under 40 bar pressure using pressure machine to increase the bond at the damaged area. Then closed the packers and needles

4. Removing the packers and cut the needles followed by grinding the surface to be rough.
5. Cleaning the surface by using air blower to remove any suspended dust.
6. After that, washing the specimen by using clean water and it was let to dry for one day.
7. A layer of primer epoxy Sikafloor® 161 (hardener and base) with 1:4 mix ratio was painted to the surface by using brush. After that, very fine sand with maximum aggregate size (0.3 - 0.6) mm was sprayed on the primer layer.
8. At last, the polyester belt was cut according to the specific dimension of the strengthening scheme. Epoxy Sikadur - 330 (base and hardener) with (4:1) mix ratio was mixed and applied to the concrete surface. Layer of polyester belt was applied to the prepared area then pressed manually by using steel roller to remove the air under the belt. Figure 3.15 briefly shows repairing the damaged specimens and resin injection

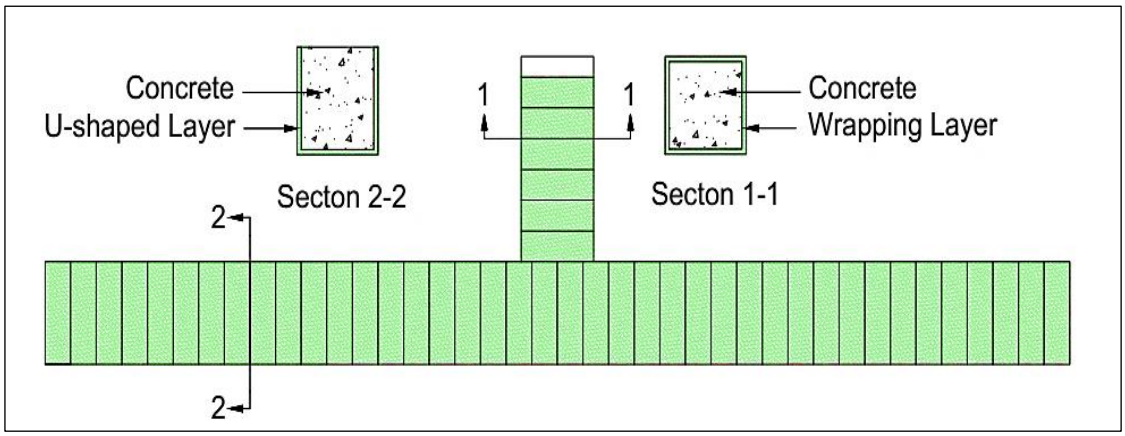

(a) Strengthening of specimen S1U

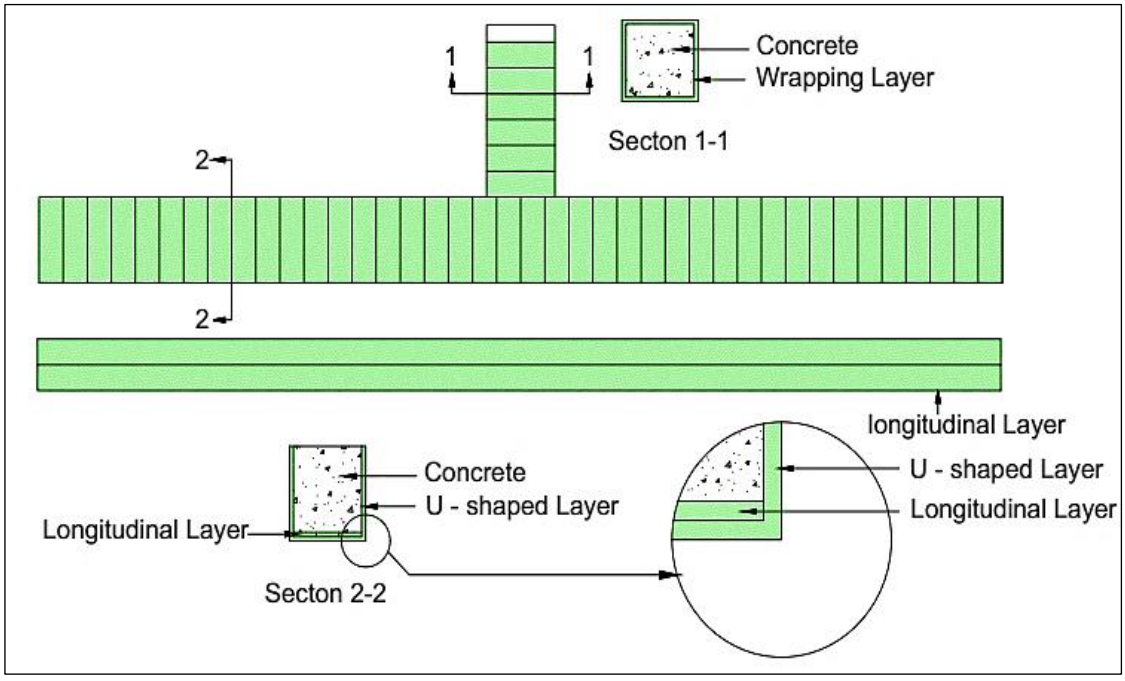

(b) Strengthening of specimen S2UL

Figure 3.12 Strengthening schemes

(a) Roughening the surface

(b) Cleaning the surface

(c) applying layer of primer epoxy

(d) Sprayed fine sand as anti-slip

(e) Cutting the polyester belt

(f) Applying strengthening scheme

Figure 3.13 Brief steps of strengthening

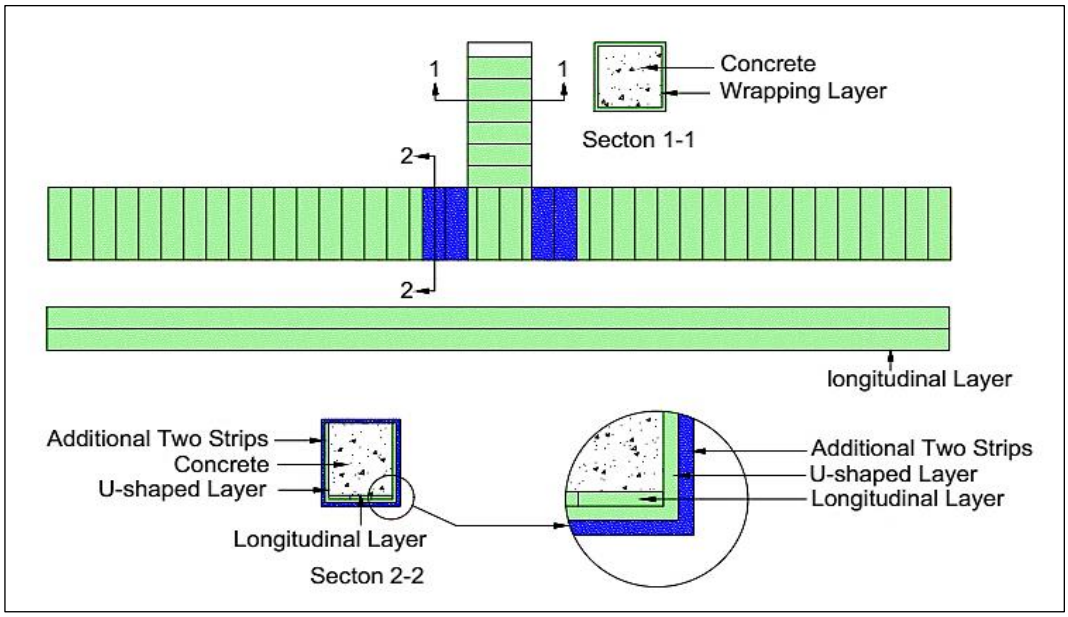

(a) Retrofitting scheme for (R1ULand R4UL) specimens

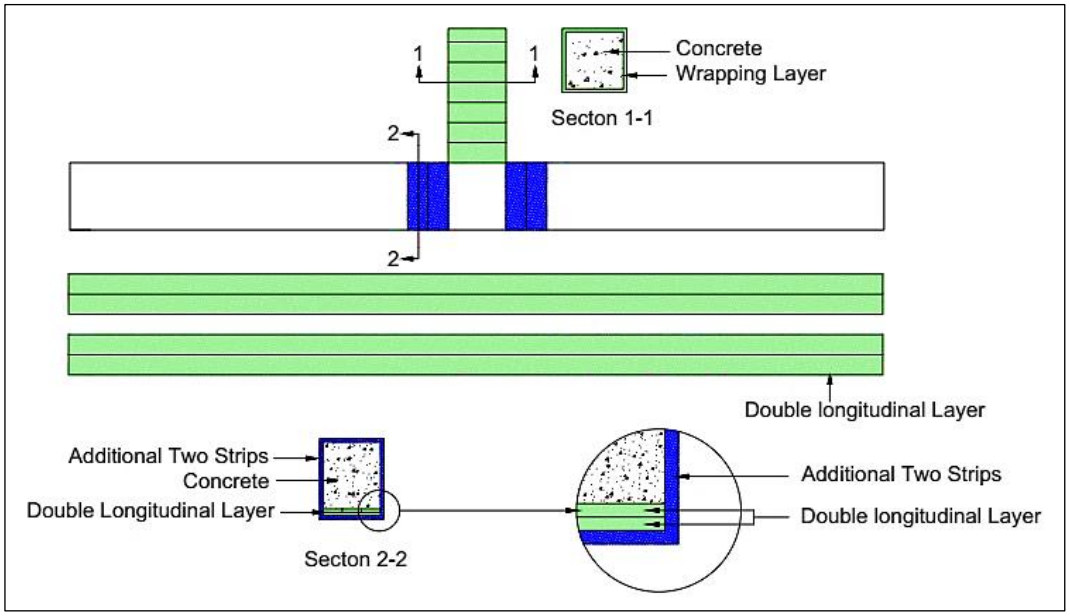

(b) Retrofitting scheme for (R2L2 and R3L2) specimens

Figure 3.14 Retrofitting schemes

(a) Install the injection needles and packers

(b) Close the cracks and damaged area around the injection needles

(c) Mixing of Sikadur - 52 LP epoxy

(d) Pressure machine

(e) Inject of the viscosity resin epoxy Sikadur - 52 LP

(f) Close the needles and packers

Figure 3.15 Injection of low viscosity resin epoxy Sikadur 52 LP

3.7 Testing of Harding Concrete

For NSC and HSC, nine concrete cubes while for SFRC fifteen concrete cubes were casted. The dimensions of these cubes were (150×150×150) mm for NSC and (100×100×100) mm for HSC and SFRC. For each concrete type, six concrete cylinders (100×200) mm in addition to three concrete prisms (100 × 100 × 500) mm were casted. These samples specimens were cured by immersing them in clean water basin for 28 days. Six concrete cubes of SFRC and three cubes of both HSC and NSC were tested at age 7 days while the remaining samples were tested at 28 days age. All the concrete cylinders and prisms for each type of concrete were tested at age of 28 day.

3.7.1 Compressive Strength Test

The concrete compressive strength test was conducted on all the concrete cubes that already were cast and cured for 28 day to determine the actual average compressive strength for each type of concrete. Figure 3.16 shows the compressive strength test.

Figure 3.16 Compressive strength test

At age of 7day, the compressive strength test was conducted on three concrete cubes of NSC and HSC while six concrete cubes were tested for SFRC at same age. The rest concrete cubes for each concrete type were tested at age of 28 day. Table 3.14 shows the obtained compressive strength from the concrete cubes at (7 and 28) days age for each type of concrete.

Table 3.14 Concrete compressive strength

Concrete type	Average Compressive Strength (7 day) (MPa)	Average Compressive Strength (28 day) (MPa)
NSC	29.4	43.0
HSC	57.95	83.2
SFRC	76.8	122.1

3.7.2 Splitting Tensile Strength Test

This test was carried out on six cylindrical samples of (100×200) mm dimensions for each type of concrete according to ASTM- C496 (ASTM, 2011b) to determinate the tensile strength of the concrete. The equation 3.1 was adopted for calculating tensile strength of concrete.

$$F_t = \frac{2P}{\pi DL} \tag{3.1}$$

where,

F_t : Concrete tensile strength (MPa)

P : Ultimate load (N)

D : Diameter of sample (mm)

L : The sample length (mm)

Figure 3.17 shows the splitting tensile test while Table 3.15 shows the results obtained for tensile strength test (MPa) for each type of concrete.

Figure 3.17 Splitting tensile strength test

Table 3.15 Splitting tensile strength results

Cylinder No.	Splitting Tensile Strength (MPa)		
	NSC	HSC	SFRC
1	2.95	5.90	10.8
2	2.87	6.10	10.7
3	3.00	5.80	10.1
4	3.10	6.00	10.5
5	3.00	5.90	10.9
6	3.00	5.91	10.8
Average	2.99	5.94	10.8

3.7.3 Flexural Strength Test

This test was achieved on three prismatic concrete samples for each type of concrete which conducted according to ASTM - C78 (ASTM, 2011a) to determine the concrete flexural strength. Three concrete prisms (100×100×500) mm for each concrete type were tested under central point load. The equation 3.2 was used for calculating the flexural strength of

concrete. Table 3.16 includes the results that were obtained from the test in (MPa) while Figure 3.18 shows the test set up and the tested specimens

$$F_r = \frac{3PL}{2bd^2} \quad (3.2)$$

where,

F_r: Concrete Flexural Strength (MPa)

P: Ultimate Load (N)

L : Span Length (mm)

b : Concrete Sample Width (mm)

d: Depth of Concrete Sample (mm)

Table 3.16 Flexural strength test results

Prism No.	Flexural Strength (MPa)		
	NSC	HSC	SFRC
1	3.51	9.00	13.53
2	3.74	8.91	13.78
3	3.58	9.08	13.69
Average	3.61	9.00	13.67

3.8 Measuring of Deflection

Dial gauge is an instrument with circular graduation measuring range of the used gauge 50 mm with 0.01 mm graduation. It was installed and set up to contact the center of the mid span area for each specimen to determinate mid span deflection. Figure 3.19 shows the dial gauge which was used during the specimen inspection.

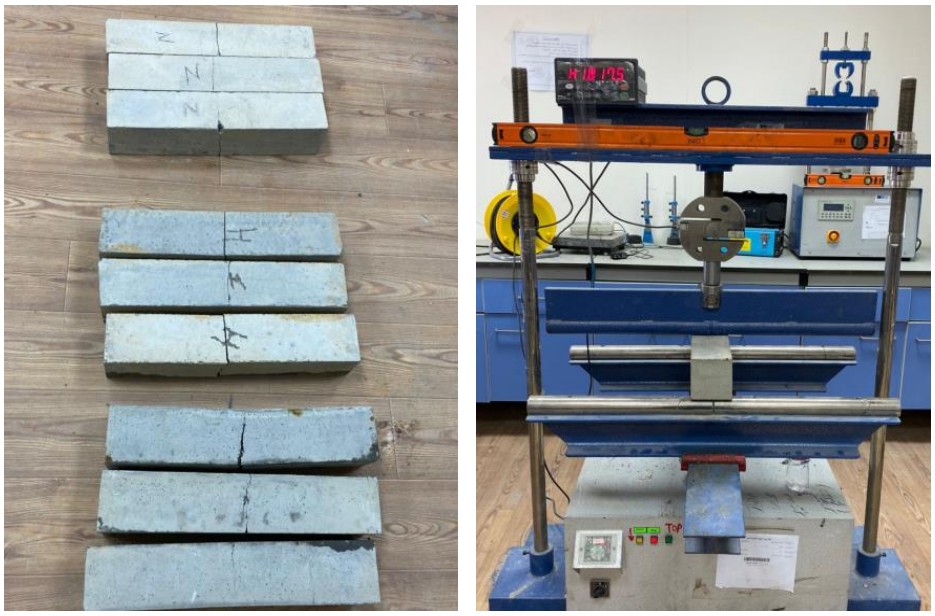

Figure 3.18 Concrete flexural strength test

Figure 3.19 Dial gauge instrument

3.9 Testing Procedure

The test was carried out to RC beam – column joint specimens at the Structural Materials Laboratory of the Technical Institute in Misan province. UTEST flexural frame test (600 kN) capacity was used for testing the specimens. The specimens were set up at the testing frame as simply

supported inverted (T-shaped). The test was applied in two stage. The first stage included testing of nine specimens up to failure (100 % damage). Two specimens were tested up to 70 % of the ultimate load of the control specimens. Downward central point load was applied from the load cell at the top of the test frame on the column face. The load increments were manually increased marking the cracks by using colored pen, recording for the reading of load. For each increment of load, concrete deflection was recorded up to failure for fully damage specimens or up to 70 % of the ultimate load for others. When the first stage of testing was ended, the strengthening and retrofitting works were started on six specimens. After completing these works, the second stage of testing was beginning. New test was conducted on two specimens which were strengthened by using polyester belt and re-test for four specimens (70 and 100) % damaged. Figure 3.20 shows simplified drawing for the test frame details. Figure 3.21 shows the frame test and the specimen set up.

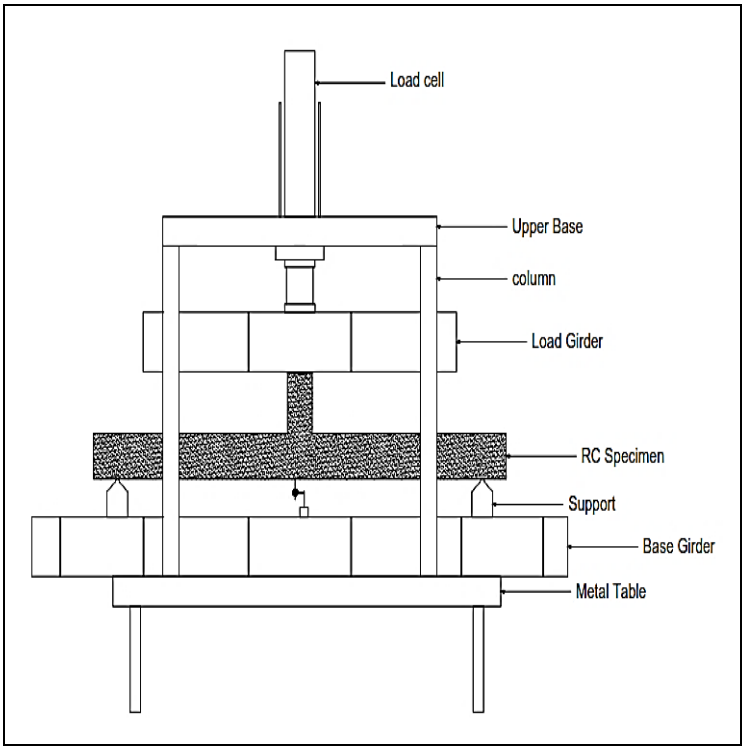

Figure 3.20 Simplified drawing for testing frame

Figure 3.21 Testing frame and specimen set up

CHAPTER FOUR

RESULTS AND DISUSSION

4.1General

All the results have been obtained from the experimental investigation of RC joint subjected to monotonic load are presented at this chapter. The test set up and the procedure of the test are the same for all the specimens. Effectiveness of the concrete compressive strength, reinforcement details in addition to strengthening and retrofitting using polyester belt are explained. The load - deflection curves are plotted and discussed in this chapter. The ductility index, toughness, initial stiffness and the load carrying capacity of the RC joint specimens are analyzed to show the effect of the suggested strengthening schemes. To study the effect of internal reinforcement details, the tested RC specimens in each group were compared to their reference specimens. Four RC specimens with conventional reinforcement details D1 were adopted as control specimens to represent three groups of concrete as listed in the Table 4.1 while to demonstrate the effect of the concrete compressive strength, specimens with the same interior reinforcement details from the groups HSC and SFRC were compared to the normal concrete NSC specimen that with the same internal reinforcement detail.

Table 4.1 Control specimens

Group	Concrete Type	Reinforcement Detail	Designation
A	NSC	D1	C1
			C2
B	HSC		H1D1
C	SFRC		F1D1

4.2 Load-Deflection Response and Ultimate Load Capacity

The deflections of all specimens are measured by a dial gauge. The dial gauge is placed at the mid span of the specimen. The test continued until the specimens reached the failure. The ultimate load verse deflection curves for each group and reinforcement details were presented in Figure 4.1 and Figure 4.2 respectively.

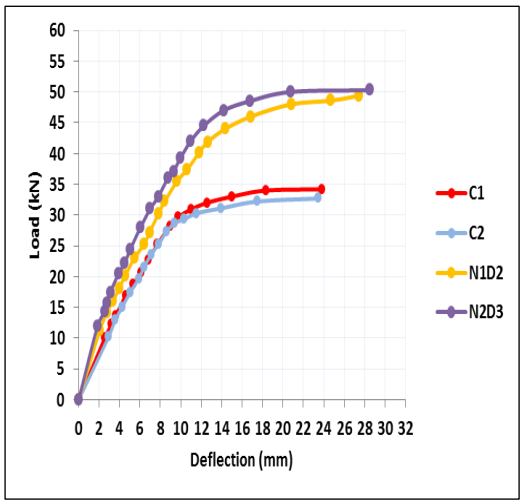

(a) Load-deflection curve of NSC

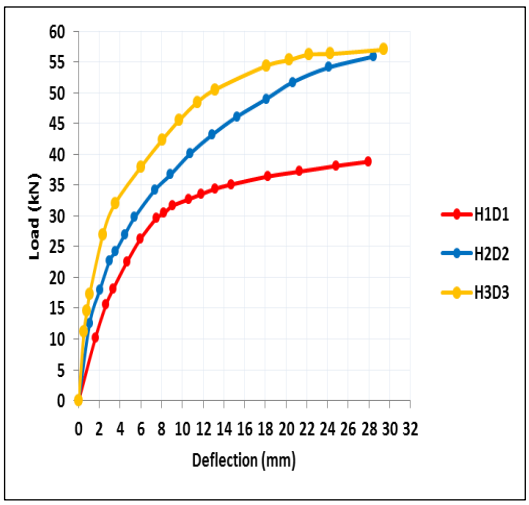

(b) Load-deflection curve of HSC

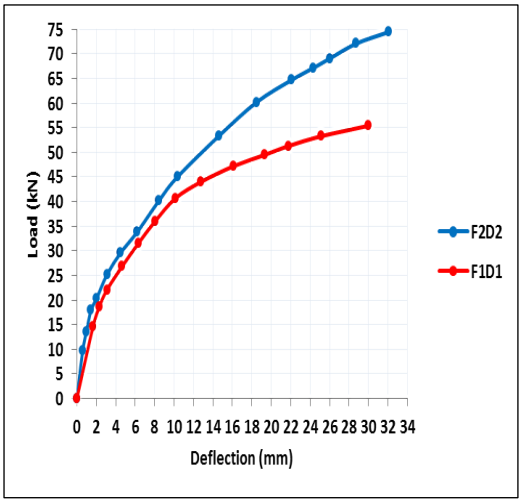

(c) Load-deflection curve of SFRC

Figure 4.1 Load - deflection curves due to reinforcement arrangement

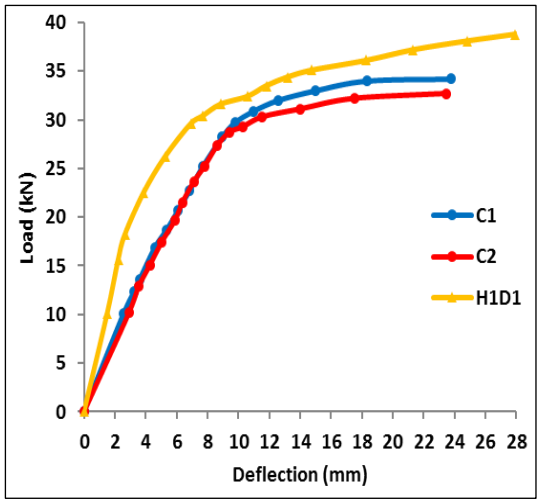

(a) Load-deflection curve of reinforcement detail D1

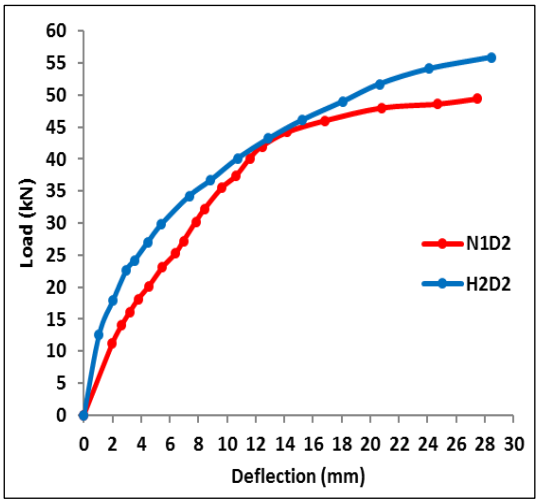

(b) Load-deflection curve of reinforcement detail D2

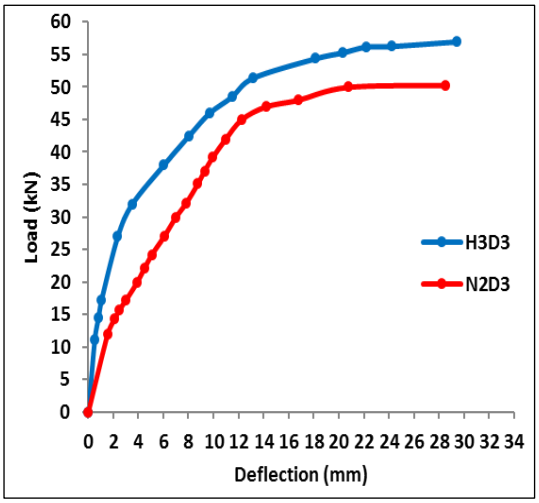

(d) Load-deflection curve of reinforcement detail D3

Figure 4.2 Load–deflection curves due to the effect of concrete compressive strength

1. In group A, the average ultimate load for the control specimens C1and C2 with conventional reinforcement detail D1 is 33.45 kN and the recorded deflection is 23.62 mm. For specimens N1D2 and N2D3 of the same group with reinforcement details D2 and D3, the ultimate loads are (49.4 and 50.3) kN with an increase by (48 and 50) %, respectively and their deflection records an increase by (16and 21) %, respectively compared to

the control specimens. Figure 4.1 shows the load - deflection curve for NSC.

2. For group B, the control specimen H1D1 of group B with reinforcement detail D1 sustained an ultimate load of 38.8 kN with mid span deflection of 27.95 mm while the remaining two specimens H2D2 and H3D3 with detail D2 and D3 recorded a maximum load of (55.9 and 57) kN with an increase by (44 and 47) % and their deflection was increased by (2 and 5) %, respectively compared to the specimens H1D1.
3. In group C, increment of (34 and 7) % in the load capacity and mid span deflection, respectively are achieved by F2D2 specimen of group C with reinforcement detail D2 compared to the control specimen F1D1 with conventional detail D1, respectively

   The ultimate load and deflection for the specimens with reinforcement detail D2 are close to those values of specimens with reinforcement detail D3 due to the arrangement of the additional internal steel around the neutral axis that derived to increase in the tensile strength and delay the first crack initiation where the confining of concrete restrained the concrete strain at the tension fiber.

4. For Reinforcement detail D1, specimen H1D1 achieved an increase of (16 and 18) % for its ultimate load and deflection, respectively while the increase ratio was (66 and 27) % for the specimen F1D1 compared with the normal concrete specimens.
5. When reinforcement detail D2 was adopted, the specimens H2D2 and F2D2 of HSC and SFRC, respectively are shown an increase in their ultimate carrying capacity and deflection comparison with the N1D2 specimen of the NSC. The specimens H2D2 and F2D2 are achieved an

increase of (13 and 51) % for the load capacity and (4 and 17) % for the deflection, respectively.

6. The increment of the ultimate load and deflection of specimen H3D3 was (13 and 3) %, respectively compared to the specimen N2D3 of NSC.

The steel fiber causes to increase the tensile strength by bridging the crack and delay the first crack load. While when the concrete compressive strength increased to 83 MPa, the flexural strength of HSC specimens and the first crack load increased too. Table 4.2 and 4.3 show the ultimate load and deflection for the tested specimens according to the reinforcement details and concrete compressive strength, respectively while Figure 4.3 shows the ultimate load sustained by the tested specimens.

Table 4.2 Ultimate load of the RC specimens due to reinforcement arrangement

Concrete Type	Reinforce-ment Detail	Designation	Deflection (mm)	% Deflection Increase	Ultimate Load (kN)	% Load Increase
NSC	D1	Average of C1 and C2	23.62	-	33.45	-
	D2	N1D2	27.48	16	49.40	48
	D3	N2D3	28.50	21	50.30	50
HSC	D1	H1D1	27.95	-	38.80	-
	D2	H2D2	28.47	2	55.90	44
	D3	H3D3	29.41	5	57.00	47
SFRC	D1	F1D1	30.00	-	55.40	-
	D2	F2D2	32.04	7	74.40	34

Table 4.3 Ultimate load of the RC specimens due to effect of concrete compressive strength

Concrete Type	Reinforce-ment Detail	Designation	Deflection (mm)	% Deflection Increase	Ultimate Load (kN)	% Load Increase
NSC	D1	Average of C1 and C2	23.62	-	33.45	-
HSC		H1D1	27.95	18	38.80	16
SFRC		F1D1	30.00	27	55.40	66
NSC	D2	N1D2	27.48	-	49.40	-
HSC		H2D2	28.47	4	55.90	13
SFRC		F2D2	32.04	17	74.40	51
NSC	D3	N2D3	28.50	-	50.30	-
HSC	D3	H3D3	29.41	3	57.00	13

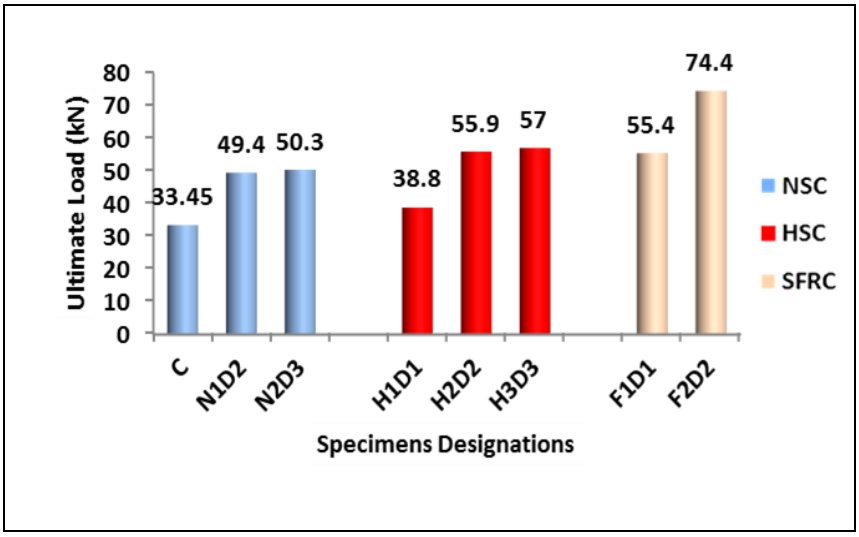

Figure 4.3 Ultimate load for the tested specimens

4.3 Initial Stiffness (IS)

The Initial stiffness of RC beam - column joint specimens is obtained depending on the relation of the load-deflection. It is equal to the slope of the line drawn from the origin passing through a point lies on the load – deflection curve opposite to 70 % of the ultimate load. This line is extended to meet a horizontal line passing through a point represents the ultimate load. Figure 4.4 explains the initial stiffness calculation (Abdulraheem, 2018). So,

$$IS = \frac{P_u}{D_y} \tag{4.1}$$

where,

IS : Initial stiffness (kN/mm)

P_u : Ultimate load at failure (kN)

D_y: Mid span deflection calculated according to Figure 4.4

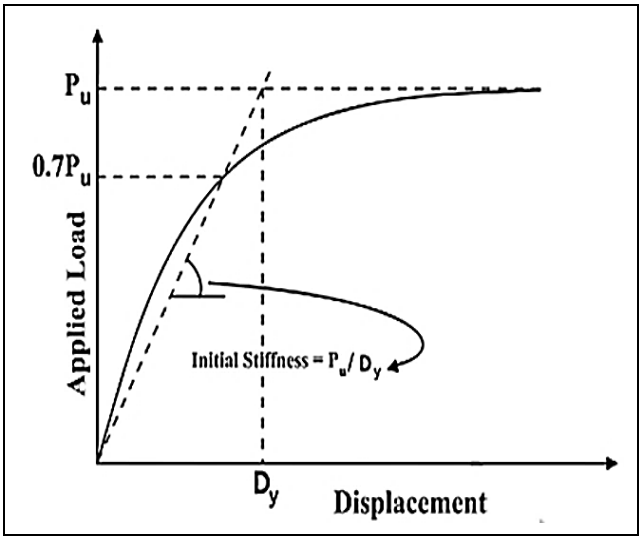

Figure 4.4 Initial stiffness calculation (Abdulraheem, 2018)

Table 4.4 and 4.5 show the initial stiffness of all the specimens of the three groups A, B and C due to reinforcement arrangement and concrete compressive strength, respectively. For NSC, an increase of (11 and 21) % for the IS of the specimens N1D2 and N2D3 with reinforcement details D2 and D3, compared to their reference with conventional detail D1, respectively. The IS of specimens H2D2 and H3D3 with reinforcement detail D2 and D3 was more than that of the control H1D1 with detail D1 by (13 and 54) %, respectively. Specimen F2D2 with detail D2 of SFRC group reordered an increase of its IS by 30 % compared to the specimen F1D1 which has detail D1 in same group. The confining using additional interior reinforcement details led to increase the initial stiffness by increasing the flexural strength. Moreover, the IS of specimens have D3 detail appeared more IS than that have D2 detail, although the two details D2 and D3 have the same amount of longitudinal and transverse reinforcement. That is, the arrangement of steel reinforcement in the beam - column joint has a vital role for enhancing the IS of RC beam - column joint.

When a high strength and steel fiber reinforced concrete used, it is observed that the IS of the HSC and SFRC is greater than that of NSC. For the first internal reinforcement detail D1, an increase in the IS of (15 and 27) % for the specimens H1D1 and F1D1, respectively compared to the NSC specimens with the same reinforcement detail D1 while the specimens H2D2 and F2D2 with reinforcement detail D2 are performed an increase of (17.5 and 49) %, respectively compared to NSC specimen N1D2 with the same detail. The specimen H3D3 of the detail D3 appeared an increasing about 48% more than that of normal concrete specimen N2D3 with the same reinforcement detail. Figure 4.5 shows the IS for all tested specimens. The enhancement of the IS is due to the increase of the flexural strength and the cracking load by increasing the concrete compressive strength.

Moreover, the specimens of SFRC had IS greater than of HSC due to using of steel fiber.

Table 4.4 Initial stiffness of the tested specimens due to reinforcement arrangement

Group	Concrete Type	Reinforce--ment Detail	Designation	D_y (mm)	P_u (kN)	I.S = P_u/D_y kN/mm	% Increase
A	NSC	D1	Average of C1 and C2	10.1	33.45	3.31	-
		D2	N1D2	13.45	49.40	3.67	11
		D3	N2D3	12.6	50.30	3.99	21
B	HSC	D1	H1D1	10.15	38.80	3.82	-
		D2	H2D2	12.96	55.90	4.31	13
		D3	H3D3	9.66	57.00	5.90	54
C	SFRC	D1	F1D1	13.2	55.40	4.19	-
		D2	F2D2	13.65	74.40	5.45	30

Table 4.5 Initial stiffness of the tested specimens due to effect of concrete compressive strength

Group	Concrete Type	Reinforce--ment Detail	Designation	D_y (mm)	P_u (kN)	I.S = P_u/D_y kN/mm	% Increase
A	NSC	D1	Average of C1 and C2	10.1	33.45	3.31	-
B	HSC	D1	H1D1	10.15	38.80	3.82	15.0
C	SFRC	D1	F1D1	13.2	55.40	4.19	27.0
A	NSC	D2	N1D2	13.45	49.40	3.67	-
B	HSC	D2	H2D2	12.96	55.90	4.31	17.5
C	SFRC	D2	F2D2	13.65	74.40	5.45	49.0
A	NSC	D3	N2D3	12.6	50.30	3.99	-
B	HSC	D3	H3D3	9.66	57.00	5.90	48.0

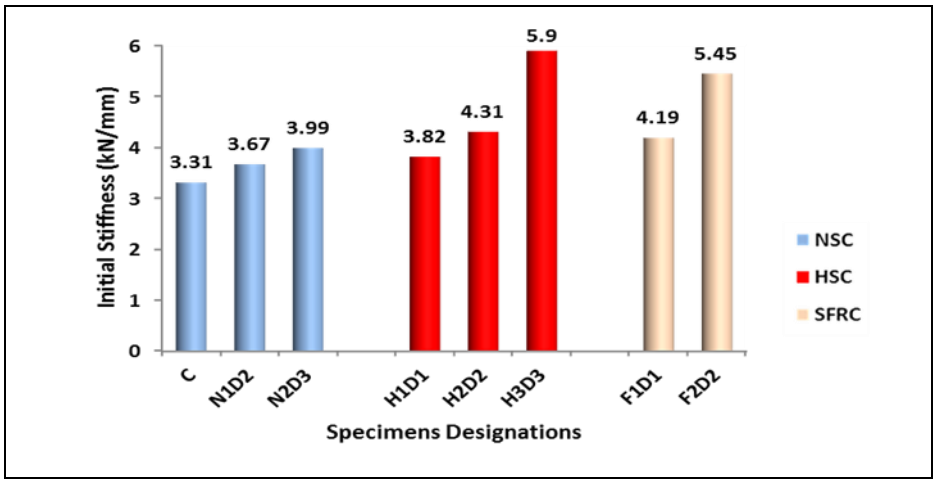

Figure 4.5 Initial stiffness of tested RC specimens

4. 4 Ductility Index

The ductility can be defined as the capability of the materials to exhibit considerable plastic deformations before reaching the breaking or rupture. The ductility index (μ) can be got depending on the load - deflection relation. It is equal to the ratio of the ultimate deflection Δu to the deflection at the yield point (Δy). So,

$$\mu = \frac{\Delta u}{\Delta y} \qquad (4.2)$$

where:

μ : ductility index (DI) (unit less)

Δu : Ultimate deflection (mm).

Δy : Deflection at the yield point (mm)

The deflection at the yield point (Δy) can be calculated from the load - deflection curve as shown in Figure 4.6 . Table 4.6 shows the ductility index of all the RC beam - column joint specimens tested in this study corresponding to the reinforcement details.

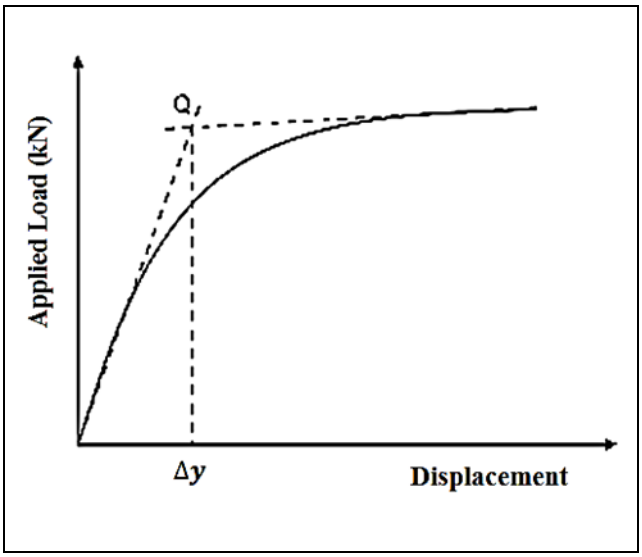

Figure 4.6 Deflection calculation at yield point (Abdulraheem, 2018)

The specimens N1D2 and N2D3 of the NSC group with reinforcement details D2 and D3 record an increase in the ductility index by (17 and 24) %, respectively compared with the reference specimens of normal detail D1. Compared to the specimen H1D1 of the HSC group with detail D1, an increase in the ductility is recorded by (27 and 74) % for the specimens H2D2 and H3D3 with D1 and D2 reinforcement details, respectively. The specimen F2D2 of the SFRC group with reinforcement detail D2 showed an increase of its ductility index by 54 % compared to the reference specimen F1D1 with reinforcement detail D1.

When high strength and steel fiber reinforced concrete are used, the ductility index for the specimens H1D1 and F1D1 of HSC and SFRC are (93 and 124) %, respectively compared to the control specimen of NSC with the same reinforcement detail D1. Also, the specimens H2D2 and F2D2 are observed an increase in ductility index of (112 and 198) %, respectively compared to the reference specimen N1D2 with same reinforcement detail D2. An increase of 131% is noticed for the specimen H3D3 of detail D3 more than the reference specimen N2D3 which has the same reinforcement detail. Table 4.7 shows the ductility index of all the

RC beam - column joint specimens tested in this study corresponding to the reinforcement details while Figure 4.7 shows the ductility index for the tested RC beam - column specimens. From the above, it is clearly noticed that using reinforcement details D2 and D3 enhanced the ductility of the tested specimens. The additional internal closed stirrups and longitudinal steel bars are arranged about the neutral axis or increasing the compressive strength contributed to the increase in the flexural and shear strength. Also, using steel fiber causes to improve the tensile strength for the concrete especially in the tensile state of the post-cracking stage. So, the specimen exhibits more bending and ductility with time under the load.

Table 4.6 Ductility index of the RC specimens due to reinforcement arrangement

Concrete Type	Designation	Ultimate Deflection Δu (mm)	Yield Deflection Δy (mm)	Ductility Index $\mu = \Delta u/\Delta y$	% Increase
NSC	Average of C1 and C2	23.62	8.65	2.73	-
	N1D2	27.48	8.70	3.16	16
	N2D3	28.50	8.50	3.35	23
HSC	H1D1	27.95	5.30	5.27	-
	H2D2	28.47	4.25	6.70	27
	H3D3	29.41	3.80	7.74	47
SFRC	F1D1	30.00	4.90	6.12	-
	F2D2	32.04	3.40	9.42	54

Table 4.7 Ductility index of the RC specimens due to effect of concrete compressive strength

Concrete Type	Designation	Ultimate Deflection Δu (mm)	Yield Deflection Δy (mm)	Ductility Index $\mu = \Delta u/\Delta y$	% Increase
NSC	Average of C1 and C2	23.62	8.65	2.73	-
HSC	H1D1	27.95	5.30	5.27	93
SFRC	F1D1	30.00	4.90	6.12	124
NSC	N1D2	27.48	8.70	3.16	-
HSC	H2D2	28.47	4.25	6.70	112
SFRC	F2D2	32.04	3.40	9.42	198
NSC	N2D3	28.50	8.50	3.35	-
HSC	H3D3	29.41	3.80	7.74	131

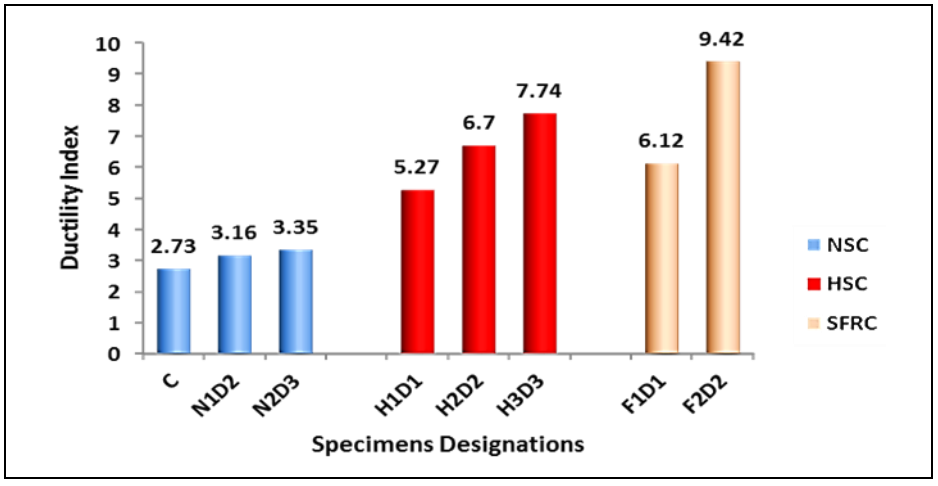

Figure 4.7 Ductility index of tested specimens

4. 5 The Energy Absorption

The energy absorption generally can be determined as the area under the load - deflection curve. Table 4.8 shows the energy absorption corresponding to the reinforcement details. The specimens N1D2 and N2D3 of NSC group with reinforcement details D2 and D3 achieved an increase in the absorbed energy of (65 and 84) %, respectively compared to the reference

specimen with normal detail D1. The increasing of energy absorption reached to (36 and 59) % for the specimens H2D2 and H3D3 of D2and D3 reinforcement details, respectively compared to the specimen H1D1 that has conventional detail D1. Moreover, the energy absorption is recorded by F2D2 of D2 reinforcement detail more than that of the control specimen F1D1 by 33% in SFRC group.

The specimens of HSC and SFRC groups record an increase in the energy absorption compared to the reference specimens of NSC that similar them by interior reinforcement details. Table 4.9 shows the absorbed energy of the RC specimens corresponding to concrete type. The specimens H1D1 and F1D1 of HSC and SFRC groups record an increase of (42 and 105) %, respectively compared to the reference specimens of NSC. The energy absorption is increased by (17 and 65) % for the specimens H2D2 and F2D2, respectively with respect to the NSC specimen N1D2. Also, the energy absorption for the specimen H3D3 of HSC is more than that of the specimen N2D3 by 23 %. The RC specimens showed an increase in the energy absorption due to concrete confining or using steel fiber led to increase the flexural and tensile strength and affect the cracking load. Using HSC or SFRC enhance the energy absorption by improving concrete strength which requires more energy accompanying the increase in the load. Figure 4.8 shows the energy absorption for the tested specimens.

Table 4.8 Absorbed energy due to reinforcement arrangement

Concrete Type	Designation	Ultimate Deflection Δu (mm)	Ultimate Load (kN)	Absorbed Energy (kN.mm)	% Increase
NSC	Average of C1 and C2	23.62	33.45	608	-
	N1D2	27.48	49.40	1005	65
	N2D3	28.50	50.30	1120	84
HSC	H1D1	27.95	38.80	863	-
	H2D2	28.47	55.90	1173	36
	H3D3	29.41	57.00	1375	59
SFRC	F1D1	30.00	55.40	1246	-
	F2D2	32.04	74.40	1657	33

Table 4.9 Absorbed energy due to effect of concrete compressive strength

Concrete Type	Designation	Ultimate Deflection Δu (mm)	Ultimate Load (kN)	Absorbed Energy (kN.mm)	% Increase
NSC	Average of C1 and C2	23.62	33.45	608	-
HSC	H1D1	27.95	38.80	863	42
SFRC	F1D1	30.00	55.40	1246	105
NSC	N1D2	27.48	49.40	1005	-
HSC	H2D2	28.47	55.90	1173	17
SFRC	F2D2	32.04	74.40	1657	65
NSC	N2D3	28.50	50.30	1120	-
HSC	H3D3	29.41	57.00	1375	23

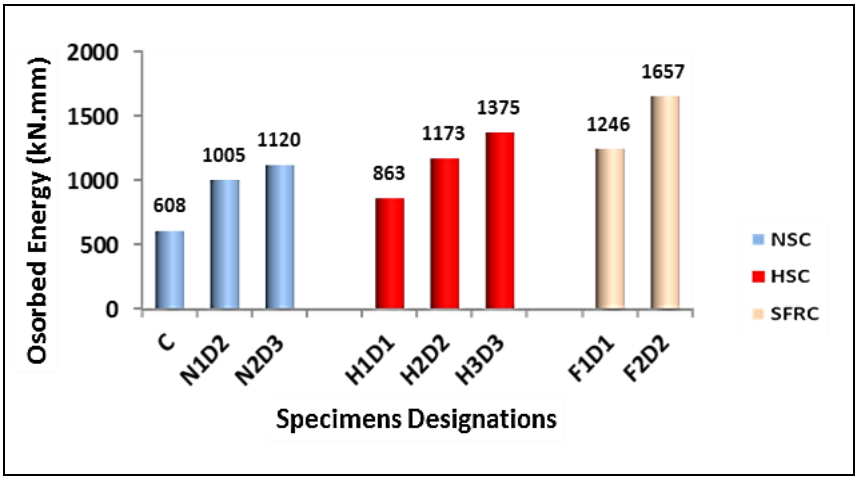

Figure 4.8 Energy absorption of the beam - column joint specimens

4.6 Strengthening and Retrofitting of RC Joint Using Polyester Belt

All the specimens that have been strengthened and retrofitted, had the same internal reinforcement detail D1 and concrete grade (normal strength concrete) but the difference between the specimens are strengthening schemes and the damage ratio (partial damage 70% or fully damage 100%). In order to study the effect of strengthening and retrofitting technique on the specimens of RC beam - column joint using polyester belt, the strengthened and retrofitted specimens are compared to the normal concrete specimens C1 and C2 "the reference specimen". Table 4.10 explained the details of all the strengthened specimens.

Table 4.10 Strengthened and retrofitted specimens' details

Original Specimen	Designation	Description	Beam	No. of layers	Column
S1U	S1U	Strengthening	U shape	1	Wrapping
S2UL	S2UL	Strengthening	U shape	1	Wrapping
			Longitudinal	1	
R1	R1UL	Retrofitting 70% damage	U shape	1	Wrapping
			Longitudinal	1	
			two trips wrapping at the face of column both sides	1	
R2	R2L2	Retrofitting 70% damage	Longitudinal	2	Wrapping
			two trips wrapping at the face of column both sides	1	
C2	R3L2	Retrofitting 100% damage	Longitudinal	2	Wrapping
			two trips wrapping at the face of column both sides	1	
C1	R4UL	Retrofitting 100% damage	U shape	1	Wrapping
			Longitudinal	1	
			two trips wrapping at the face of column both sides	1	

4.6.1 Load - Deflection Response and Load Capacity

The average ultimate load and deflection of the tested RC joint specimens (reference) C1 and C2 are 33.45 kN and 23.63 mm as shown in Table 4.11 . Figure 4.9 represents the load - deflection curve for the strengthened and retrofitted specimens.

1. A significant increase for the ultimate load capacity for the specimen S1UL where the maximum load and deflection for this specimen are 61.5 kN and 38.45 mm, respectively. The increment of the ultimate load and deflection of S1UL are (84 and 63) % compared to the reference specimens, respectively.
2. The retrofitting is applied to the specimens R1UL and R2L2 that are tested up to 70% the ultimate load of the reference specimens. The retrofitting schemes are applied to specimens and then reloaded them. A noteworthy increase in the load carrying capacity and deflection for four retrofitted specimens compared to the unstrengthen control specimens.
3. The increment in the load capacity compared with the control specimens are (96,109, 85 and 79) % for the specimens R1UL, R2L2, R3L2 and R4UL, respectively. Also, the deflection of these specimens was increased by (110, 70, 19 and 73) %, respectively.
4. Clear to notice the effect of longitudinal strengthening layers where it restored and increased the load capacity for the specimens by increase their flexural strength and the first crack loads. Moreover, the retrofitting technique for partial damage tested specimens up to 70% of ultimate load is more efficiency than that of fully damage (100% up to failure load) athough the schemes of retrofitting are similar. The micro cracks at the concrete specimens R1UL and R2L2 do not slightly effect on the flexural strength and the reinforcement steel does not yielded yet. So, the load is

resisted by all together in addition to polyester belt while the load of the specimens R3L2 and R4UL is sustained by the repaired concrete and the polyester belt. Figure 4.10 shows the ultimate load of the strengthened and retrofitted specimens.

Table 4.11 Ultimate load and deflection of strengthened and retrofitted specimens

Designation	Ultimate Load (kN)	% Load Increase	Maximum Deflection (mm)	% Deflection Increase
Average of C1 and C2	33.45	-	23.63	-
S1U	36.15	8	30.20	28
S2UL	61.50	84	38.45	63
R1UL	65.50	96	49.60	110
R2L2	69.80	109	40.22	70
R3L2	62.00	85	28.23	19
R4UL	60.00	79	40.80	73

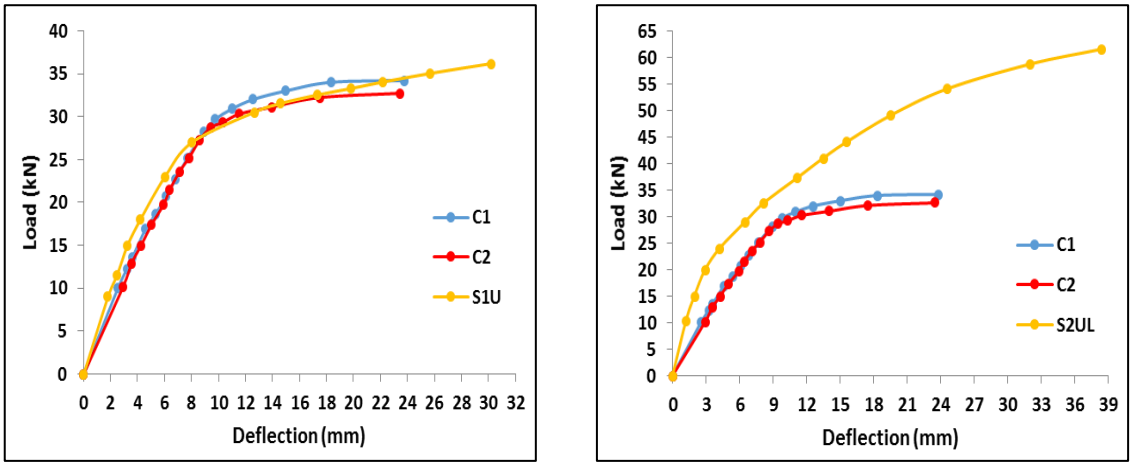

(a) S1U (b) S1UL

Figure 4.9 Load - deflection curve for strengthened and retrofitted specimens

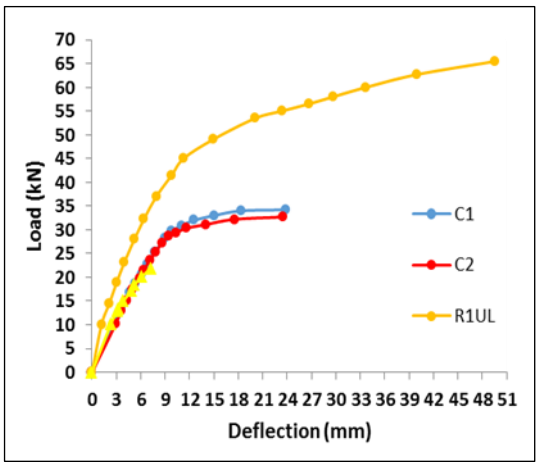

(c) R1UL

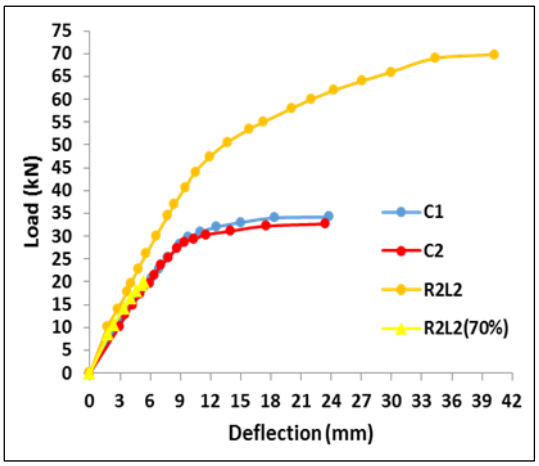

(d) R2L2

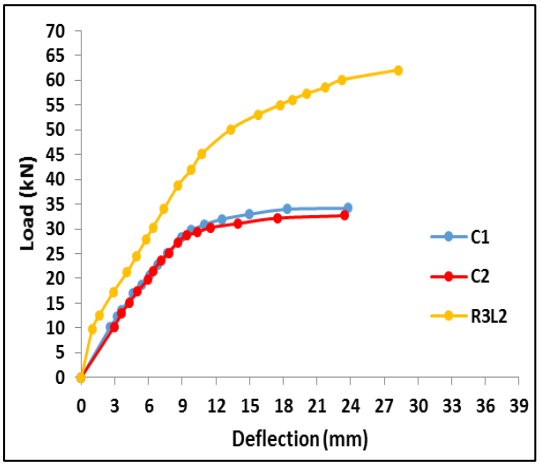

(e) R3L2

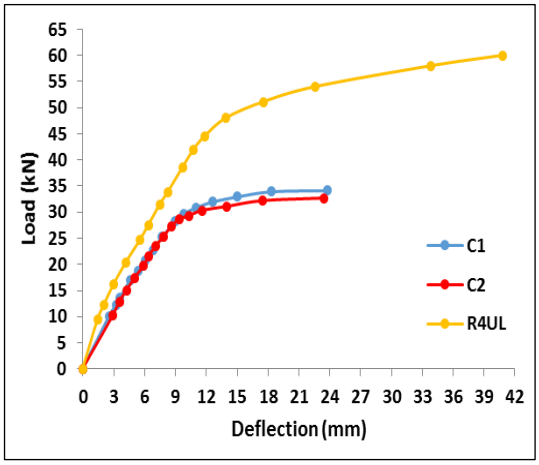

(f) R4UL

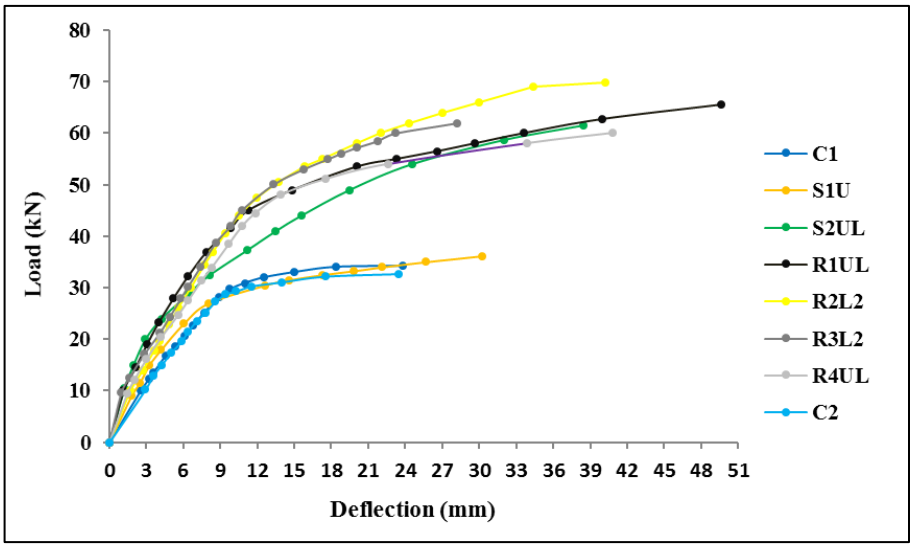

(g) Strengthened and Retrofitted specimens Compared to Control

Figure 4.9 : Continued

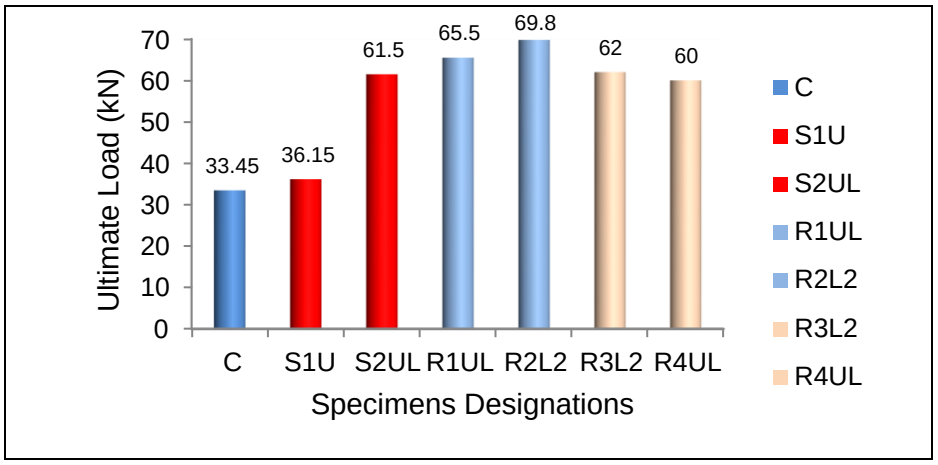

Figure 4.10 Ultimate load of strengthened and retrofitted specimens

4.6.2 Initial Stiffness

The initial stiffness of the RC specimens (controls, retrofitted and strengthened) is listed in Table 4.12 . It is observed from the results that the specimen S1U is showed little increase in its initial stiffness 9 % compared to the control. Its strengthening scheme (U-shaped) did not significantly affect. The specimen S2UL recorded noticeable increase in its initial stiffness due to the effect of presence longitudinal layer. It recorded 26% increase than the control specimen. The specimens R1UL and R2L2 showed a close in their initial stiffness, but the initial stiffness of these specimens is more than of S1U due to using a longitudinal layer of polyester belt that is led to increasing the flexural strength of the RC joint. But this increase is limited to be less than other specimens as a result of the micro cracks that are appeared during the first test before retrofitting. The increments of the initial stiffness for the specimens are (16 and 15.8) %, respectively compared to the reference specimens. The specimen R3L2 is showed the largest increase of the initial stiffness due to the use of a double longitudinal layer of bolster belt in addition to the compressive strength of the resin epoxy that has been injected. The increase of initial stiffness is 28% compared to the reference specimens.

An increase of initial stiffness for the specimen R4UL is recorded 17% compare to the control specimens. It is less than the strengthened specimen S2UL due to the yielding of the reinforcement steel and the load is resisted just by the longitudinal layer and the repaired concrete in specimen R4UL. Figure 4.11 shows the initial stuffiness of retrofitted and strengthened specimens.

Table 4.12 Initial stiffness of strengthened and retrofitted specimens

Designation	D_y (mm)	P_u (kN)	I.S = P_u/D_y kN/mm	% Increase
Average of C1 and C2	10.1	33.45	3.31	-
S1U	9.98	36.15	3.62	9
S2UL	14.75	61.50	4.17	26
R1UL	17	65.50	3.85	16
R2L2	18.22	69.80	3.83	15.8
R3L2	14.6	62.00	4.24	28
R4UL	15.5	60.00	3.87	17

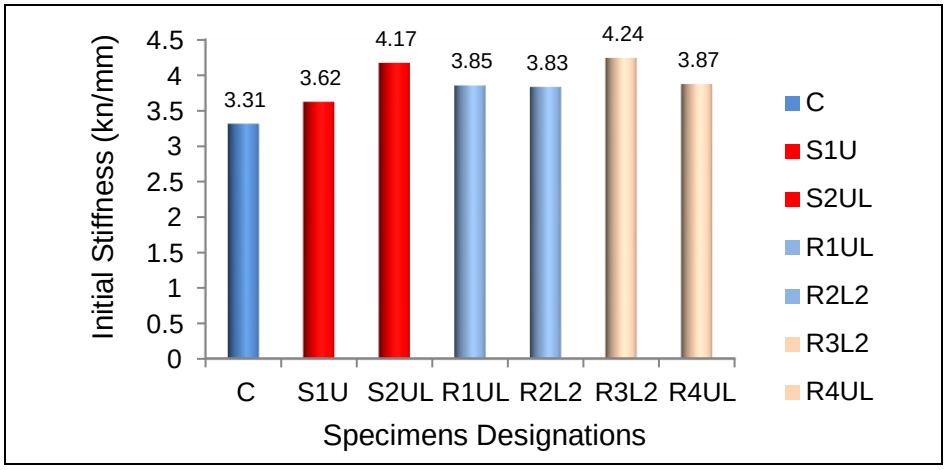

Figure 4.11 Initial stiffness of strengthened and retrofitted specimens

4.6.3 Ductility Index

It is observed that the ductility index for the retrofitted and strengthened specimens using schemes that consisted of a single layer of

polyester belt are greater than of other specimens due to increasing flexural strength. Except for the specimen R4UL due to yielding of the steel reinforcement in the first test before applying the retrofitting. The specimens R1UL, S2UL and R4UL achieved an increase in its ductility index by (145, 117 and 81) %, respectively compared to the reference specimens. While the increments of the ductility index were (47, 97 and 74) % for the specimens R2L2, R3L2 and S1U, respectively. Table 4.13 and Figure 4.12 show the ductility index for the strengthened and retrofitted specimens.

Table 4.13 Ductility index of strengthened and retrofitted specimens

Designation	Ultimate Deflection Δu (mm)	Yield Deflection Δy (mm)	Ductility Index $\mu = \Delta u/\Delta y$	% Increase
Average of C1 and C2	23.62	8.65	2.73	-
S1U	30.20	6.35	4.75	74
S2UL	38.45	6.50	5.92	117
R1UL	49.60	7.40	6.70	145
R2L2	40.22	10.00	4.00	47
R3L2	28.23	5.25	5.37	97
R4UL	40.8	8.25	4.95	81

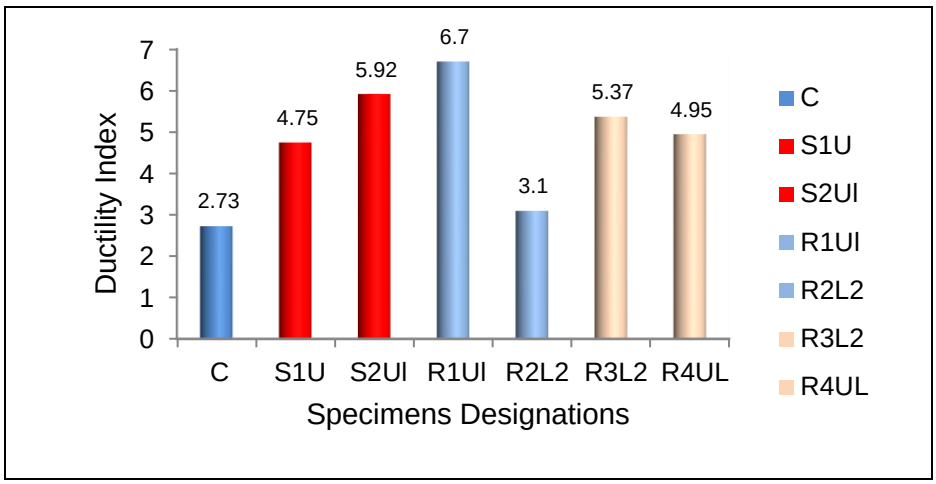

Figure 4.12 Ductility index of strengthened and retrofitted specimens

4.6.4 Energy Absorption

The absorbed energy for all the retrofitted and strengthened specimens are listed in Table 4.14 . The increment of energy absorption for the specimens R1UL, R4UL and S2UL are (315, 210 and 181) %, respectively compared to the reference specimens. This development is due to using a strengthening scheme include U-shaped in addition to longitudinal layer of polyester belt which led to increase the shear and flexural strength. The specimen R2L2 also achieved a significant increase of 240 % as a result of using double layers of polyester belt. In addition, the increase is due to the concrete and steel reinforcement of the specimen still not reach to its yield. Also, the adhesive material affect the tensile strength of the specimen through seal all the cracks generated in the specimen. The increase ratio of the energy absorption for the specimen R3L2 which repaired after full damage is 106% compared with reference member. The increment of energy absorption of specimen R3L2 is smaller than that of R2L2. That is due to the specimen R3L2 was fully damaged and then retrofit by using epoxy injection and polyester belts. The specimen S1U achieves an increase of its absorbed energy by 40 % with respect to the control. Figure 4.13 shows the energy absorption for strengthened and retrofitted specimens.

Table 4.14 Energy absorption for strengthened and retrofitted specimens

Designation	Absorbed Energy (kN.mm)	% Increase
Average of C1 and C2	608	-
S1U	852	40
S2Ul	1707	181
R1Ul	2521	315
R2L2	2067	240
R3L2	1255	106
R4UL	1882	210

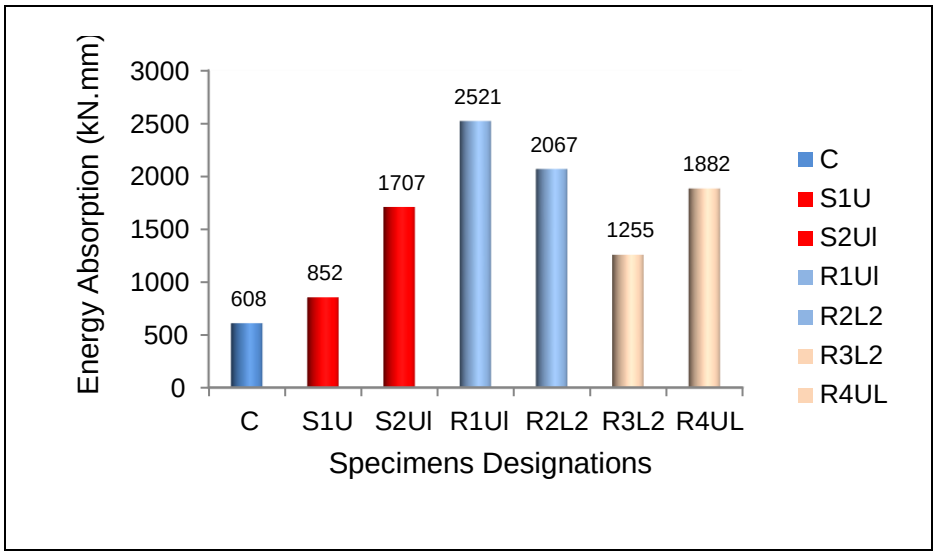

Figure 4.13 Absorbed Energy for strengthened and retrofitted specimens

4.7 Crack Pattern and Failure Mode

The overall cracks pattern that observed for all tested specimens are flexural cracks. Several cracks began to appear as micro-cracks. These cracks formed firstly due to different loads corresponding to the type of concrete, reinforcement detail and strengthening or retrofitting techniques. They have been derived from the extreme fiber of the tension zone and took a vertical direction toward the compression zone. Then, these cracks were increased and expanded in addition to developing other cracks with the increase in the applied load to the tested specimen. The main cracks in the specimens that have reinforcement detail D2 and D3, are formed approximately at the edge of the additional internal reinforcement. Moreover, the number of cracks is increased too. For the normal concrete specimens, the first cracks load for the control specimen C1 and C2 which are closed as 13.6 and 12.9 kN, respectively. As for the specimens N1D2 and N2D3 that have reinforcement details D2 and D3 respectively, the number of the cracks was more than that of the control specimens which has conventional reinforcement detail D1. The addition steel leads to increase the tensile strength of the specimens. That means, the first cracks loads are

increased. Therefore, it noticed the cracking load of specimens N1D2 and N2D3 20.1 and 22.2 kN, respectively for the specimens N1D2 and N2D3, respectively. When the flexural strength of the specimens increased due to increasing the concrete compressive strength, the first crack load also increased. The cracks at the HSC specimens began to appear at the extreme fiber of the tension zone at the loads 18.2, 24.2 and 27 kN for the specimens H1D1, H2D2 and H3D3, respectively. The crack load of the SFRC was also increased. The cracking loads are 36.5 and 40.2 kN for the specimens F1D1 and F2D2, respectively. The Figure 4.14 shows the crack patterns of the RC beam - column joint which were divided according to their concrete type. Unclear crack pattern of the strengthened or retrofitted specimens consists of (U-shaped layer) while the cracks at the retrofitted specimens do not have this layer, the cracks also appeared at the edge of the longitudinal layers as well as to the additional strips. The number of cracks for the specimens R3L2 is more than that of the specimen R2L2 due to the epoxy resin that is injected to the specimen R3L2. Moreover, the micro - cracks that are formed at the specimen R2L2 for the first testing before applying the retrofitting scheme. Figure 4.15 shows the crack patterns of strengthened and retrofitted specimens. Crushing of concrete is also observed at the top region of the compression zone for the normal concrete specimens adjacent to the column face or near to the additional strips in strengthened specimens as shown in Figure 4.16 . The failure mode of all the tested specimens is a flexural failure due to confining and the additional steel arrangement in the specimens. The crushing of concrete is observed at the top region around the column face or additional polyester strips due to increasing the tensile strength as a result for the longitudinal layers of the polyester belts. Through testing the retrofitted and strengthened specimens, it did not observe debonding between the polyester belts and concrete substrates. Also, the rupturing of

polyester belts is noticed. That indicates the efficiency of the strengthening technique used in this study.

(1) Crack Patterns of C1

(2) Crack Patterns of C2

(3) Crack Patterns of N1D2

(4) Crack Patterns of N2D3

(a) Crack patterns of normal strength concrete specimens

(1) Crack Patterns of H1D1

(2) Crack Patterns of H2D2

(3) Crack Patterns of H3D3

(b) Crack patterns of high strength concrete specimens

Figure 4.14 Crack patterns of RC Specimens according to concrete type

	
(1) Crack Patterns of F1D1	(2) Crack Patterns of F2D2

(c) Crack patterns of steel fiber reinforced concrete specimens

Figure 4.14: Continued

	
(1) Specimen S1U	(2) Specimen S2UL
	
(3) Specimen R1UL	(4) Specimen R2L2
	
(5) Specimen R3L2	(6) Specimen R4UL

Figure 4.15 Crack Patterns of strengthened and retrofitted specimens

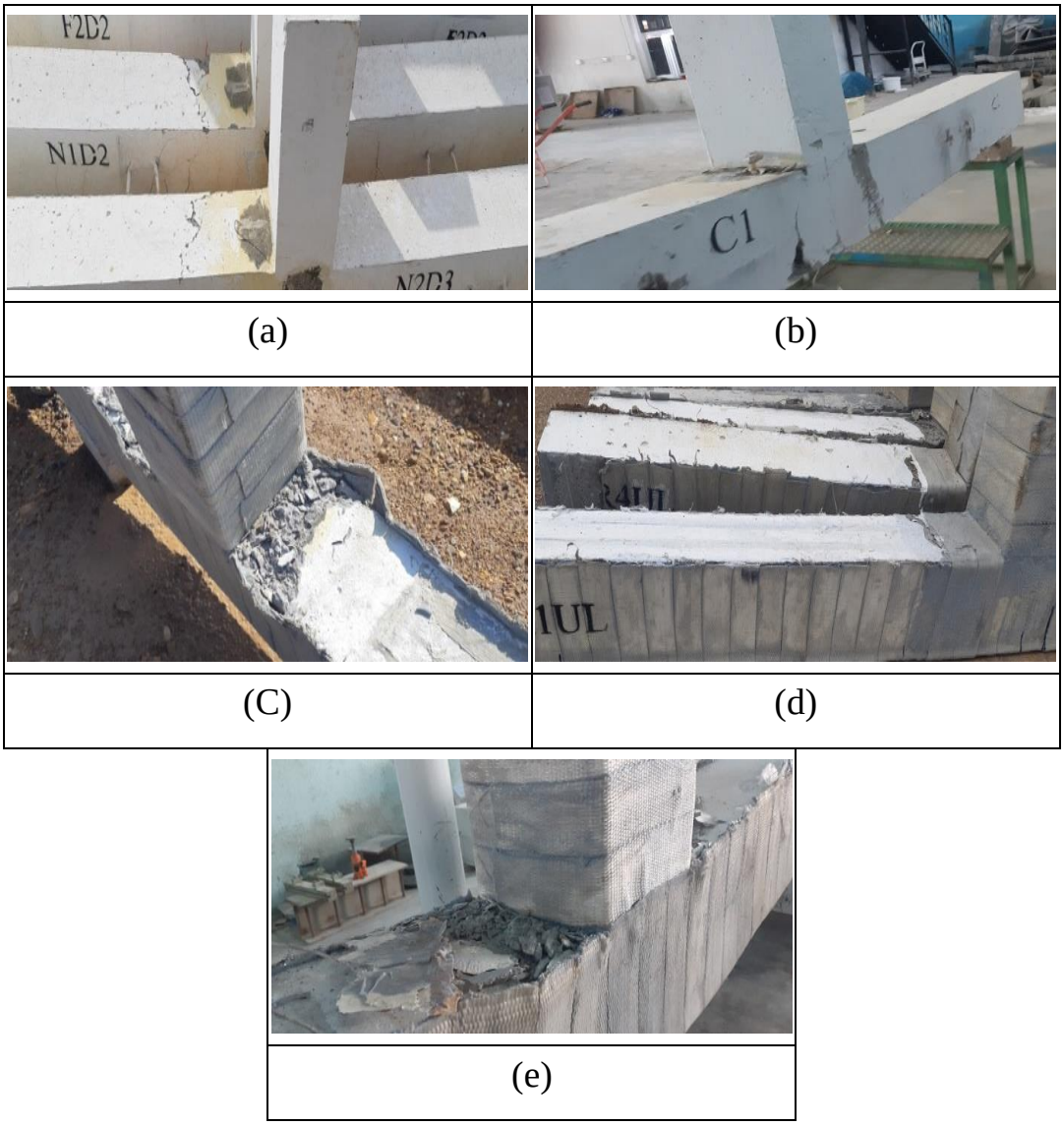

(a) (b)

(C) (d)

(e)

Figure 4.16 Concrete Crushing

CHAPTER FIVE

CONCLUSIONS AND RECOMMENDATIONS

5.1 Conclusions

All the RC beam - column joint specimens are tested under a monotonic load. Based on the conducted test results, the following conclusions are drawn.

1. The loads carrying capacities of the tested specimens are improved for the specimens due to using reinforcement detail D2 and D3.
2. Increasing the load carrying capacity for the tested specimens as a result of increasing the concrete compressive strength.
3. The strengthening or retrofitting of exterior RC beam-column joint by using polyester belt as a new suggested technique has significantly increased the load carrying capacity.
4. The U-shaped layer of polyester belt that have been applied to the strengthened specimen has a little effect on the load carrying capacity where it works to increase the shear strength of the specimens.
5. Retrofitting technique by using polyester belt has significant effect to restore and improve the capacity of the damaged RC beam - concrete joint with different failure levels.
6. Increasing the number of the polyester belt layers from one to two layers does not affect the load carrying capacity. Compared to the retrofitted specimens consisting of one belt layer with damage ratio (70 and 100) %, the increase ratio was (6.5 and 3.3) % for the specimens with two layers and same damage ratio, respectively. Using more than one layer with HSC or SFRC may increase the ultimate load capacity.

5.2 Recommendations for Further Studies

Suggested recommendations to be taken into consideration in the future Studies:

1- Numerical modeling for the RC joint specimens and the results to be compared with the experimental results.
2- Investigating different retrofitting and strengthening schemes to choose the optimum one that achieves further increase in the load capacity of the RC beam - column joint.
3- Investigating the behavior of hybrid RC beam column joint using steel fiber.
4- Applying the strengthening and retrofitting schemes on the (high strength and steel fiber reinforced) RC joint specimens, also, using more than one layers for strengthening.
5- investigating the effect of new suggested retrofitting technique by using polyester belt on the non-seismic joint.
6- Investigating the brittle failures of the beam – column joint (both shear and bond slip).

REFERENCES

Abdulghani, A.W. and Jaafer, A.A., 2021. Comparative Numerical Study between/Steel Fiber Reinforced Concrete and SIFCON on Beam-Column Joint Behavior. In Materials Science Forum (Vol. 1021, pp. 138-149). Trans Tech Publications Ltd.

Abdulraheem, M. S. (2018). Experimental investigation of fire effects on ductility and stiffness of reinforced reactive powder concrete columns under axial compression. *Journal of Building Engineering, 20*, 750-761.

ACI Committee 363-2010 Report on High-Strength Concrete. American Concrete Institute.

Akash S., Jayasree S. (2018). Effect of Near Surface and Externally Bonded Retrofitting on Exterior Beam-Column Joint. *International Journal of Engineering and Advanced Technology (IJEAT), 8*(4C).

Arowojolu, Ibrahim, Rahman, Al-Osta and Al-Gadhib. Plastic hinge relocation in reinforced concrete beam–column joint using carbon fiber–reinforced polymer. *Advances in Structural Engineering*. 2019 Oct; 22(14), 2951-2965.

ASTM. (2005). Standard Specification for Chemical Admixtures for Concrete: American Society for Testing and Materials.

ASTM. (2011a). Standard Test Method for Flexural Strength of Concrete (Using Simple Beam With Center-Point Loading). In A. S. f. T. o. Materials (Ed.): American Society for Testing of Materials.

ASTM. (2011b). *Standard test method for splitting tensile strength of cylindrical concrete specimens*: American Society for Testing Material / International.

ASTM (Ed.) (2003). *Standard Specification for Silica Fume Used in Cementitious Mixtures*. US: American Society for Testing and Materials.

Attari, N., Amziane, S., and Chemrouk, M. (2010). Efficiency of beam–column joint strengthened by FRP laminates. *Advanced Composite Materials, 19*(2), 171-183.

Azarm, R., Maheri, M. R., and Torabi, A. (2017). Retrofitting RC joints using flange-bonded FRP sheets. *Iranian Journal of Science and Technology, Transactions of Civil Engineering, 41*(1), 27-35.

Balaji, S., and Thirugnanam, G. (2017). Study on exterior RC beam-column joints upgrade with SIFCON in joint core under reversed cyclic loading. *KSCE Journal of Civil Engineering, 21*(1), 346-352.

Bansal, P. P., Kumar, M., and Dar, M. A. (2016). Retrofitting of exterior RC beam-column joints using ferrocement jackets. *Earthquakes and Structures, 10*(2), 313-328.

Behbahani, H., Nematollahi, B., and Farasatpour, M. (2011). Steel fiber reinforced concrete: A review. International Conference on Structural Engineering, Construction and Management (ICSECM-2011), Kandy, Sri Lanka.

Bindhu, K., Mohana, N., and Sivakumar, S. (2016). New Reinforcement Detailing for Concrete Jacketing of Nonductile Exterior Beam–Column Joints. *Journal of Performance of Constructed Facilities, 30*(1), 04014192.

Binti Abd Kader, A. N., Osman, S., and Yatim, M. (2019). A State-Of-The-Art Review on Retrofitting Beam-Column Joint Using GFRP with NSM Technique under Seismic Loading. *International Journal of Engineering and Technology, 11*(1).

Iraqi Standard No. 5 /1984. Physical and chemical requirements for portland cement.

Iraqi Standard No. 45 /1984. Requirements of the used fine and coarse aggregate in the concrete mixes.

Iraqi Standard No. 2091/1999 Carbon steel bars for the reinforcement of concrete, (1999).

ACI-ASCE Committee 352 - (2002). Recommendations for Design of Beam-Column Connections in Monolithic Reinforced Concrete Structures.

Das, P., and Choudhury, S. (2018). Experimental Study on Fibre-Reinforced Concrete Beam-Column Joint with Ductile Detailing Under Reverse Cyclic Loading. *International Journal of Engineering & Technology, 7*(3.16), 85-89.

DCP. (2019). *Hperplast PC260 MSDA and TDS*. Retrieved from Lebanon:

Gokdemir, H.,and Tankut, T. (2017). Seismic Strengthening of Beam-Column Joints Using Diagonal Steel Bars. *Teknik Dergi, 28*(3), 7977-7992.

Fangueiro, Raul . Fibrous and composite materials for civil engineering applications. Woodhead publishing, 2011.

Ha, G.-J., and Cho, C.-G. (2008). Strengthening of reinforced high-strength concrete beam–column joints using advanced reinforcement details. *Magazine of concrete research, 60*(7), 487-497.

Hadi, M. N., and Tran, T. M. (2016). Seismic rehabilitation of reinforced concrete beam–column joints by bonding with concrete covers and wrapping with FRP composites. Materials and Structures, 49(1), 467-485.

Hassan, W., Park, S., Lopez, R., Mosalam, K., and Moehle, J. (2010). *Seismic response of older-type reinforced concrete corner joints.* Paper presented at the Proceedings, 9th US National Conference and

10th Canadian Conference of Earthquake Engineering, Toronto, Canada, paper.

Hassouna, F., and Jung, Y. W. (2020). Developing a Higher Performance and Less Thickness Concrete Pavement: Using a Nonconventional Concrete Mixture. *Advances in Civil Engineering, 2020*.

Kannan, P., Sivakumar, S., and Bindhu, K. (2013). Seismic strengthening of exterior RC beam - column joints by advanced ferrocement jacketing. *Int. J. Innovat. Res. Sci., Eng. Tech, 2*(1), 53-58.

Le-Trung, K., Lee, K., Lee, J., Lee, D. H., and Woo, S. (2010). Experimental study of RC beam–column joints strengthened using CFRP composites. *Composites Part B: Engineering, 41*(1), 76-85.

Mahmoud, M. H., Afefy, H. M., Kassem, N. M., and Fawzy, T. M. (2014). Strengthening of defected beam–column joints using CFRP. *Journal of advanced research, 5*(1), 67-77.

Misir, I., and Kahraman, S. (2013). Strengthening of non-seismically detailed reinforced concrete beam–column joints using SIFCON blocks. *Sadhana, 38*(1), 69-88.

Montava, I., Irles, R., Pomares, J. C., and Gonzalez, A. (2019). Experimental Study of Steel Reinforced Concrete (SRC) Joints. *Applied Sciences, 9*(8), 1528.

Montava, I., Irles, R., Segura, J., Gadea, J.M. and Juliá, E., 2019. Numerical simulation of steel reinforced concrete (SRC) joints. Metals, 9(2), p.131

Mostofinejad, D., and Akhlaghi, A. (2017). Experimental investigation of the efficacy of EBROG method in seismic rehabilitation of deficient reinforced concrete beam–column joints using CFRP sheets. *Journal of Composites for Construction, 21*(4), 04016116.

Panesar, D. K. (2019). Supplementary cementing materials. In Developments in the Formulation and Reinforcement of Concrete (pp. 55-85). Woodhead Publishing.

Revanth Jagana, C. V. K. (2017). High strength concrete. *International journal of engineering sciences and research technology, 3*. doi:DOI: 10.5281/zenodo.291853

Sharbatdar, M. K., Kheyroddin, A., and Emami, E. (2012). Cyclic performance of retrofitted reinforced concrete beam–column joints using steel prop. *Construction and Building Materials, 36*, 287-294.

Sika. (2020a). *Product Data Shee / Sikadur-52 LP*. Retrieved from Product Data Shee / Sikadur-52 LP:

Sika. (2020b). *Product data sheet*. Retrieved from Product data sheet \ Sikadur- 31 CF Slow:

Sika. (2020c). *Ptoduct data sheet*. Retrieved from Ptoduct data sheet \ Sikadur-330:

Singh, V., Bansal, P. P. G., Kumar, M. G., and Kaushik, S. (2015). *Retrofitting of reinforced concrete beam-column joints using bonded laminates*. (Doctoral dissertation).

Torabi, A., and Maheri, M. R. (2017). Seismic repair and retrofit of RC beam–column joints using stiffened steel plates. *Iranian Journal of Science and Technology, Transactions of Civil Engineering*, *41*(1), 13-26.

Uma, S., and Prasad, A. M. (1996). Seismic behavior of beam column joints in reinforced concrete moment resisting frames. *Document No.: IITK-GSDMA-EQ32-V1. 0, Final Report: A-Earthquake Codes, IITK-GSDMA Project on Building Codes*.

Wang, G.-L., Dai, J.-G., and Bai, Y.-L. (2019). Seismic retrofit of exterior RC beam-column joints with bonded CFRP reinforcement: An experimental study. *Composite Structures*, *224*, 111018.

Appendix A

Design of RC joint specimen

f_y = 420 MPa $f_c^{`}$ = 35 Mpa

Rectangular cross section for beam b_{beam} = 170 mm h_{beam} =200 mm

Square cross section for column b = h = 170 mm

$$\beta = 0.85 - \frac{0.05(f_c^{`} - 28)}{7} = 0.85 - \frac{0.05(35-28)}{7} = 0.8$$

$$\rho_{max} = 0.364\,\beta\,\frac{f_c^{`}}{f_y} = 0.364 \times 0.8 \times \frac{35}{420} = 0.0242$$

$$\rho_{min} = \frac{\sqrt{f_c^{`}}}{4f_y} = \frac{\sqrt{35}}{4 \times 420} = 0.0035$$

$As_{min} = \rho_{min} bd$, b = 170mm , d = 200 - (2×10+6+10/2)= 169 mm

$As_{min} = 0.0035 \times 170 \times 169 \cong 100\ mm^2$

Use $\phi 10\ mm$ ⇨ No. of $\phi 10$ = 100/79 =1.27 ≅ 2

As = 2× 79 = 158 mm^2 ρ = 158/(170×169) = 0.005

Mu = $\phi\rho bd^2 f_y(1 - 0.59\rho f_y/f_c^{`})$

$$=0.9 \times 0.0055 \times 170 \times 169^2 \times 420\ \left(1 - 0.59 \times 0.005 \times \frac{420}{35}\right) \times 10^{-6}$$

$$\cong 10\ kN.m$$

$$P_u = 4\,\frac{M_u}{l_n} \quad , l_n = 2\ m \quad \Rightarrow P_u = 20\ kN$$

$$V_u = \frac{P_u}{2} = 10\ kN \Rightarrow \frac{V_u}{\phi} = \frac{10}{0.85} = 11.76\ kN$$

$$V_c = \frac{\left(0.16\lambda\sqrt{f_c^{`}} + 17\,\rho\frac{V_u d}{M_u}\right) bd}{7} \leq 0.29\sqrt{f_c^{`}}\,bd$$

$\lambda = 1\ for\ normal\ concrete$

$$\frac{V_u d}{M_u} = 0.169 < 1$$

$$V_c = \frac{\left(0.16\sqrt{35} + 17 \times .005 \times 0.169\right) \times 169 \times 17010^{-3}}{7} = 4\ kN$$

$$V_s = \frac{V_u}{\phi} - V_c = 11.76 - 4 = 7.76\ kN$$

$\frac{1}{3}\sqrt{f_c`}\ bd = 56.65\ kN$ ⇨ $V_s < \frac{1}{3}\sqrt{f_c`}\ bd$

$S = \frac{A_v\ f_y\ d}{V_s}$ Use ϕ 6 mm as closed stirrups two legs ⇨$S = 523\ mm$

$$S_{max} = \min of\ \frac{d}{2}\ , 3\frac{A_v f_y}{b}$$

$S_{max} = 84.5\ , 375$ ⇨ $S_{max} = 84.5mm$

$S > S_{max}$, $Use\ S_{max} = 70\ mm$

To achieve penetration of concrete through the steel bars and to ensure vibrating for the concrete when using internal closed stirrups use S=140 mm

For column

$P_u = \phi \times 0.8[0.85f_c`\left(A_g - A_{st}\right) + f_y A_{st}]$

$A_g = 170 \times 170 = 289000\ mm^2$

$A_{st} = A_g \times \rho_g$ $let\ \rho_g = 0.01$

$A_{st} = 28900 \times 0.01 = 289\ mm^2$

Use $\phi 10\ mm$ ⇨ No. of $\phi 10$ = 289/79 =3.65 ≅ 4

$S_{max} = 16db = 160\ , 48dt = 288, last\ dimension\ of\ column = 170$

$S_{max} = 160$ $use\ S_{max} = 120\ mm$

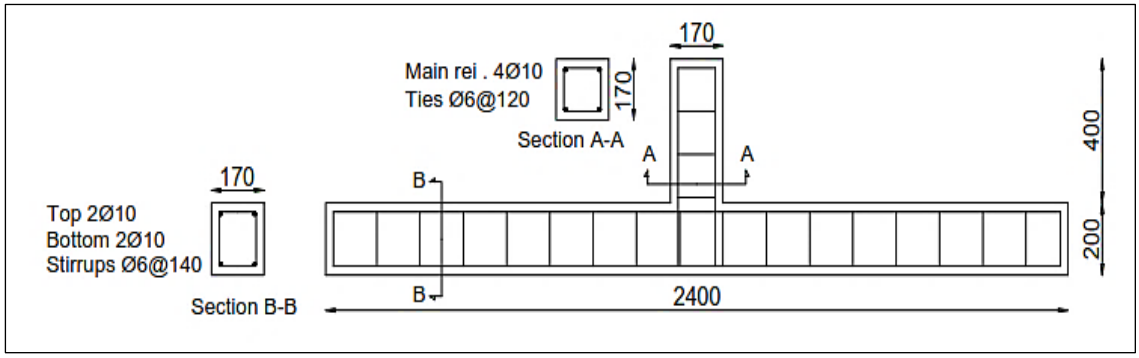

й НыЬ Ю

في هذه الدراسة ، تم اعتماد تقنية جديدة مقترحة لتقوية وإعادة تأهيل المفاصل الخرسانية المسلحة باستخدام أربطة البوليستر. تهدف هذه الدراسة إلى معرفة تأثير تقييد ومقاومة إنضغاط الخرسانة على المفاصل الخرسانية المسلحة. وكذلك دراسة ثأثير تقوية و إعادة تأهيل المفاصل الخرسانية باستخدام أربطة البوليستر. تم استخدام ثلاثة نماذج مختلفة من تفاصيل حديد التسليح استخدمت في تجهيز وصب النماذج حيث يمثل النموذج الاول التسليح العادي النموذجي ، النموذج الثاني مشابه للنموذج الاول مع اضافة حديد تسليح داخلي طولي محاط بأترية داخلية مغلقة ضمن منطقة المفصل بينما النموذج الثالث مماثل للنموذج الثاني الا ان الاترية الأضافية الداخلية تكون مزدوجة اي في منطقة الشد ومنطقة الضغط . أيضاً تم استخدام ثلاثة أنواع من الخرسانة وهي الخرسانة ذات المقاومة العادية ، عالية المقاومة والخرسانة المقواة بالألياف الفولاذية ذوات مقاومات الأنضغاط 43 ، 83 و 122 ميجاباسكال على التوالي. تم اجراء الفحص على خمسة عشر نموذجاً من المفاصل الخرسانية المسلحة . تم فحص النماذج على شكل حرف (T) مقلوب تحت تأثير حمل مفرد وباتجاه واحد حيث تم تسليط الحمل عموديًا باتجاه الأسفل على وجه العمود. تم اجراء التقوية واعادة التاهيل باستخدام أربطة البوليسترحيث تم تطبيق نمطي التقوية على نموذجين بينما نمطي اعادة التاهيل فقد تم تطبيقهما على أربعة نماذج بنسب تضرر مختلفة (70 و 100) %.

أوضحت نتائج الاختبار أن استخدام تفاصيل التسليح مع الأترية الداخلية أو الأترية الداخلية المزدوجة زاد من سعة الأحمال القصوى لنماذج المفاصل الخرسانية المسلحة مقارنة بتفاصيل التسليح العادية حيث كانت الزيادة (47 و 50)٪ على التوالي للخرسانة العادية ، و (44 و 47)٪ الخرسانة عالية المقاومة و 34٪ للخرسانة المقواة بالألياف الفولاذية. بزيادة مقاومة الانضغاط للخرسانة ، إزدادت سعة الاحمال القصوى للنماذج لكل من الخرسانة المقواة بالالياف والخرسانة ذات المقاومة العالية مقارنة بالخرسانة العادية لكل تفصيل من تفاصيل التسليح الحاوي على أترية داخلية مغلقة. كانت نسبة الزيادة للخرسانة عالية القوة والخرسانة الليفية بتفاصيل التسليح العادية (16 و 66)٪ على التوالي ، لتفاصيل التسليح الحاوية على أترية داخلية مغلقة كانت الزيادة (13 و 51)٪ على التوالي وعند اعتماد التسليح الحاوي على اترية داخلية مزدوجة تم تحقيق زيادة بنسبة 13٪ للخرسانة ذات المقاومة العالية مقارنة بالخرسانة العادية.

نتيجة لاستخدام أربطة البوليستر في تقوية نموذجين وإعادة تأهيل اربعة نماذج من المفاصل الخرسانية المسلحة تم اختبارها مسبقاً بنسب تضرر (70و 100) % ، زادت قدرة تحمل الأحمال القصوى للنماذج بشكل كبير بنطاق (79 إلى 109) ٪ مقارنة بالعينات غير المقواة.

جمهورية العراق
وزارة التعليم العالي والبحث العلمي
جامعة ميسان / كلية الهندسة
قسم الهندسة المدنية

تقوية وإعادة تأهيل المفاصل الخرسانية المسلحة باستخدام أربطة البوليستر

رسالة
مقدمة الى كلية الهندسة في جامعه ميسان
كجزء من متطلبات نيل درجة الماجستير في علوم الهندسة المدنية/ انشاءات

من قبل

ضياء جاسب رشك

بكالوريوس هندسة مدنية 2002

نيسان 2021

باشراف

الأستاذ الدكتور عبد الخالق عبد اليمه جعفر